ORCA – Online Research @ Cardiff

This is an Open Access document downloaded from ORCA, Cardiff University's institutional repository:https://orca.cardiff.ac.uk/id/eprint/138034/

This is the author's version of a work that was submitted to / accepted for publication.

Citation for final published version:

Naeem, Abdul, Kerr, Andrew C. , Kakar, Muhammad Ishaq, Siddiqui, Rehanul Haq, Khan, Muhammad Ayoub and Ahmed, Nisar 2021. Petrology and geochemistry of volcanic and volcanoclastic rocks from Zhob ophiolite, North-Western Pakistan. Arabian Journal of Geosciences 14 (2) , 97. 10.1007/s12517-020-06352-0

Publishers page: http://dx.doi.org/10.1007/s12517-020-06352-0

Please note:
Changes made as a result of publishing processes such as copy-editing, formatting and page numbers may not be reflected in this version. For the definitive version of this publication, please refer to the published source. You are advised to consult the publisher's version if you wish to cite this paper.

This version is being made available in accordance with publisher policies. See http://orca.cf.ac.uk/policies.html for usage policies. Copyright and moral rights for publications made available in ORCA are retained by the copyright holders.

Petrology and Geochemistry of Volcanic and Volcanoclastic Rocks from Zhob Ophiolite, North-Western Pakistan

Abdul Naeem[1&3], Andrew C. Kerr[2], Muhammad Ishaq Kakar[3], Rehanul Haq Siddiqui[4], Muhammad Ayoub Khan[3], Nisar Ahmed[1]

[1]*Geological Survey of Pakistan, Quetta, Pakistan*
[2]*School of Earth and Ocean Sciences, Cardiff University, Main Building, Park Place, Cardiff, Wales CF10 3AT, UK 2*
[3]*Center of Excellence in Mineralogy, University of Baluchistan, Quetta, Pakistan*
[4]*BUITEMS, Baluchistan University of Information Technology, Engineering and Management Sciences, Quetta, Pakistan*

Corresponding Author E-mail: ayoub.cemuob@gmail.com

Abstract

The Zhob ophiolite is divided into Ali Khanzai, Omzha, and Naweoba blocks. The ophiolite geology comprises various lithological units including basalt chert and hyaloclastite mudstone units. The basalt chert and hyaloclastite mudstone units consist of thick lava and pelagic sediments. On the basis of petrology and geochemistry the lavas of basalt chert unit can be divided into tholeiitic basalt, trachy-basalt, basaltic andesite and dacite and that of hyaloclastite mudstone unit into more alkaline foidite, picro-basalt and tephrite-basanite. The tholeiitic rocks have a flat N-MORB normalized pattern with enrichment of Th and depletion of Nb compared to other immobile elements and thus indicate a subduction zone component in the rocks. They have chondrite-normalized REE patterns typical of N-MORB. The alkaline rocks have depleted chondrite-normalized HREE compared to N-MORB similar to those of OIB. Our geochemical results suggest that the tholeiitic rocks may have formed in a supra subduction zone setting while the alkaline rocks are intraplate setting that was influenced by a subduction component. The Zhob lavas therefore are likely to represent the floor of a branch of the Ceno-Tethys Ocean and may have obducted over the Indian Plate passive continental margin during Late Cretaceous.

Key Words: Ophiolite, volcanic rocks, volcanoclastic rocks, petrogenesis, tectonic setting.

1. Introduction

The composition of volcanic (basaltic) lava can provide reliable evidence as to the tectonic setting of ophiolites due to their distinctive geochemical characteristics of ophiolites in specific tectonic settings (Pearce and Cann 1973; Pearce et al. 1984; Xia and Li 2019). The geochemical characteristics of volcanic rocks indicates that associated ophiolites can be generated can be formed in a variety of tectonic settings (Dilek and Furnes 2011, 2014).

The most significant ophiolites appear to have formed in supra-subduction zone (SSZ) environments (Pearce et al. 1984; Shervais 2001; Pearce 2003; Whattam and Stern 2011). SSZ ophiolite lavas have geochemical signatures that range from mid-ocean ridge basalt (MORB) to volcanic arc basalt (VAB) and include those formed in back-arc basins and intra-arc basins in addition to those formed during subduction initiation (Pearce 1982).

In Pakistan, the ophiolite complexes occur along the northern and western sutures of the Indian plate with the Afghan block (Tapponnier 1981). The important ophiolite bodies are Bela-Zhob Valley-Waziristan ophiolites which demarcate the western boundary of Indian plate with Afghan block (Gansser 1979). Among these ophiolites the Muslim Bagh and Waziristan ophiolites (south and north of Zhob ophiolite, respectively) are well studied and are of supra-subduction zone origin (Kakar et al. 2014; Khan et al. 2001).

The less-well studied Zhob ophiolite is part of the Waziristan-Zhob Valley-Bela ophiolite suture zone and is a Mesozoic sedimentary-igneous complex which can be divided into three ophiolitic blocks, namely: The Ali Khanzai, Newaoba, and Omzha blocks (Jones 1961; Fig. 1). The ophiolite is highly deformed and dismembered and due to it being thrusted onto the passive continental margin sediments of the Indian plate (Jones 1961, Ahmed et al. 2020). The Naweoba is the largest of the blocks and is located to the north of Zhob town while the other two blocks are found to the south of the Naweoba block (Fig. 1). Volcanogenic massive sulfide and manganese ores are currently being mined in the Naweoba and Ali Khanzai blocks (Khan, 2020). This study discusses the field features, petrography, and geochemistry of the Zhob Ophiolite to determine its petrogenesis and tectonic setting.

2. Regional and Local Geology

The ophiolites of Pakistan occur in western and northern ophiolitic belts. The Zhob Ophiolite is a part of the western ophiolite belt (Fig. 1) comprising the Waziristan, Zhob valley and Bela ophiolites, which occupy the suture zone between the Afghan block and Indian plate (Gansser 1979). The rocks of the Zhob Ophiolite, unconformably overlie the early Triassic-Eocene sediments of calcareous zone, which are in turn overlain by flysch type sandstone interbedded with mudstone and limestone of flysch zone (Iqbal and Shah 1980). The flysch zone is part of a large Katwaz sedimentary basin (Treloar and Izatt 1993) that represents a fluvial to shallow marine depositional environment. The stratigraphic succession of this zone from oldest to youngest rocks is: Nisai Formation, Khojak Formation, Dasht Murgha group, Malthanai Formation and Bostan Formation (Kasi et al. 2012). The underlying rocks of the ophiolite; the calcareous zone, comprises early Jurassic to Paleocene rocks including the Walgai Formation, the

Shirinab Formation, the Parh Group, the Mughal Kot Formation and the Dungan Formation (Warraich et al. 1995) (Fig. 1).

Zhob ophiolite is a part of Zhob valley ophiolites that consists of three ophiolitic bodies exposed near and named after the localities of Khanozai, Muslim Bagh and Zhob. The Waziristan ophiolite is located in the north of the studied area, and although it is dismembered it contains well-exposed mantle, crustal sections and upper volcano-sedimentary units (Khan 2000). The Waziristan ophiolite suggests formation in a back-arc basin setting (Khan et al. 2001), Muslim Bagh ophiolite, in the south of Zhob Ophiolite, is another well-exposed and well-developed ophiolite that contains almost all ophiolitic rock units; mantle section, transition zone, crustal section and lava and at its base, and a has also a well exposed metamorphic sole rock (Kakar 2012). The ophiolite of Muslim Bagh was formed in a back-arc basin setting (Siddiqui et al. 1994, Kakar et al. 2014). While the Bela ophiolite is generated in a supra-subduction zone setting (Ahmed 1991, 1993).

The Zhob ophiolite is highly deformed and dismembered and is thrusted onto the passive continental margin sediments of the Indian plate (Jones 1961). It comprises three separated blocks; Ali Khanzai, Omzha and Naweoba blocks (Fig. 1). These three blocks of the Zhob Ophiolite have been divided into various rock units (Fig. 2a, b, c) that are reviewed below. The crustal plutonic unit (Zcp), is mainly composed of both layered and massive gabbros and the fine-grained cumulate gabbros. The olivine gabbros are present at the base to norite-gabbro norite and hornblende gabbros at the top of the unit. The mantle section unit (Zms), is composed of dunite, harzburgite, lherzolite, wehrlite and pyroxenite. The metamorphic unit (Zmr), is mainly composed of amphibolite, green schist and chlorite schist facies rocks. The basalt chert unit (Zbc), is composed of thick pillow lava associated with bedded chert, pelagic limestone, hyaloclastite and hemi-pelagic mudstone. The hyaloclastite mudstone unit (Zhm), is comprised of basaltic rocks interbedded with limestone and siliceous mudstone. The upper sedimentary unit (Zus) is composed of siliceous and fissile shale interbedded with micritic limestone, while the lower sedimentary unit (Zls) is composed of siliceous and flaky shale with argillaceous limestone. The Zbc and Zhm units are described in detail below.

3. Analytical methods

Thin sections for the petrographic studies were prepared in the thin section cutting laboratory of the petrology and mineralogy department laboratory of the Geological Survey of Pakistan, Quetta. The slab saw was used for the chipping of large samples and the trim saw was used to further minimize their thickness. The chips were then ground with silicon carbide and polished with a polisher to make the 0.03mm thick sections. The thin sections were covered with coverslip by using the Canada balsam. The thin sections were studied in the petrology and mineralogy laboratory of the Geological Survey of Pakistan, Quetta and Center of Excellence in Mineralogy, University of Balochistan, Quetta, by using the Olympus optical transmitting light microscope.

Twelve rocks samples of volcanic rocks for major, trace and rare earth elements were analyzed from the three ophiolitic bodies of the Zhob ophiolite. After removing the weathered surfaces, the samples were crushed in a jaw crusher and then powdered by using agate ball mill to the size of 200 mesh or less. Each sample of two grams' powder was then heated to obtain the loss on ignition in a porcelain crucible to 900°C for two hours. The major, trace and rare earth elements were analyzed by using (ICP-OES) and (ICP-MS) at Cardiff University, Wales, UK.

A lithium metaborate fusion method was used for ICP analysis in the rocks samples study. In a platinum crucible, the samples were prepared, each ignited sample of 0.1g was mixed with 0.4g of lithium metaborate flux. In each mixture, a few drops of wetting agents such as lithium iodide were added for fusion by using the Claisse Fluxy automated fusion system. By using the Milli-Q purification system the mixture was then dissolved in 20ml of 10% HNO_3 and 30ml of de-ionized water. 1ml of 100 ppm Rh spike was added to the solution when the mixture had fully dissolved and the solution was made up to 100ml with 20 de-ionized water. To determine the major element and some trace element abundances 20ml of each solution was run on ICP-OES. 1ml of each solution was added to 1ml of In and Tl and 8ml of 2% HNO_3, to determine the abundances of trace element, was run on ICP-MS. A thermos elemental X7 series ICP-MS and a JY von Horiba Ultima 2 ICP-OES instruments at Cardiff University Wales, UK were used to analyze element abundances.

4. Results

4.1. Field Features of Volcanic and Volcanoclastic Rocks of Zhob Ophiolite

The field features of the volcanic and volcanoclastic rocks of the Ali Khanzai block, Omzha block and Naweoba block of the Zhob Ophiolite are described together in the sections below.

4.1.1. Basalt Chert Unit (Zbc)

Thick outcrops of the basalt chert unit (Zbc) with similar lithological characteristics are exposed in Ali Khanzai, Naweoba and Omzha blocks of Zhob ophiolite. This unit forms large ridges and covers about 60% area of

Ali Khanzai, 50% of Omzha and 40% of the Naweoba blocks (Fig. 2a, b, c). The unit is composed of thick pillow lava associated with red chert, pelagic and hemipelagic limestone and mudstone. The pillows are 12 centimeters to 1.5 meters in diameter and are porphyritic and amygdaloidal in texture (Fig. 3a). The basalt chert unit is fragmented and is in thrust contact with peridotite and crustal gabbroic rocks, and the doleritic dykes intrude the ultramafic rock unit (Fig. 3b). In the basalt chert unit, the basalts are interbedded with multi- and red-colored, medium to thick-bedded chert and limestone. The red chert forms large hills and is abundant in the mapped area (Fig. 3c). In several localities of in the Naweoba block e.g., Kaza Khowra, the basalt contains some of economic minerals such as iron, copper, and manganese. While in the Ali Khanzai block manganese is being locally mined (Khan et al. 2020). Copper in the Zhob ophiolite occurs in the form of malachite, azurite and chalcopyrite (Khan 2020).

At its base, the basalt chert unit of the Naweoba block is in thrusted contact with the ultramafic and mafic rock unit (Fig. 3c). In places, the hyaloclastite mudstone unit is thrust over the basalt chert unit example near Khozakzai Killi, north of the Naweoba block (Fig. 3c) and incorporates large blocks of metamorphic rocks, probably amphibolite, forming high mountain peaks (Fig. 3d).

4.1.2. Hyaloclastite Mudstone Unit (Zhm)

The hyaloclastite mudstone unit (Zhm) is found in all three blocks of the Zhob ophiolite and covers about 50% of the area of Naweoba, 40% of Ali Khanzai and 30% of the Omzha block (Fig. 2a, b, c). In the Ali Khanzai and Omzha blocks, the upper part of this unit is comprised of basaltic rocks with limestone and siliceous mudstone while the lower and middle part of the unit it is comprised of limestone and shale. In the studied area, the Zhm has is in thrust contact with the mafic-ultramafic unit which are in turn thrust over sedimentary rock (Fig. 4a). The amygdaloidal and vesicular structures of the basalt are filled with zeolite, calcite, and secondary quartz (Fig. 4b). These amygdaloidal and vesicular structures are abundant and can be observed in all ophiolitic blocks of the Zhob ophiolite. The tuff and fragments of volcanic, ultramafic, mafic and sedimentary rocks were observed in the hyaloclastite mudstone unit of the Zhob ophiolite (Fig. 4c-d).

In the Naweoba block, the upper part of this unit contains basaltic rocks with minor hemipelagic mudstone and limestone while in the lower and middle parts, the basaltic rocks overlap with sedimentary rocks. In some places in the Naweoba block, the hyaloclastite mudstone unit is thrusted over the ultramafic and mafic rock unit while in other places, it is thrusted over the basalt chert unit. In the Ali Khanzai and Omzha blocks, this unit is in thrust contact with the mafic and ultramafic rock, the basalt chert and with sedimentary rock units. A lenticular body of deformed pillow basalt within the volcanoclastic rock is exposed near the Killi Ismail Bagh Esazai area of the Naweoba block. The hyaloclastite mudstone unit is thrusted back over the upper sedimentary rock unit in the northeast of the Naweoba block. In the Zhob ophiolite, the hyaloclastite mudstone unit is distributed all over the blocks with thick outcrops forming massive hills.

4.2. Petrography

The Zhob Ophiolite basalt consists of plagioclase and clinopyroxene minerals as phenocrysts while the groundmass is predominantly clinopyroxene and plagioclase with minor chlorite and epidote (Fig. 5). They are fine-grained and show aphanitic, hemi crystalline, inequigranular, porphyritic and sub ophitic textures. Basalt in the Zbc unit is partially to completely altered and shows sub-porphyritic to sub-ophitic textures with a micro-crystalline to coarse-grained crystal size. The plagioclase constitutes more than 65 percent of the rock by the volume and present both in the form of phenocrysts as well as fine radiating micro-laths in groundmass. The phenocrysts of plagioclase are largely altered and occur in a micro to cryptocrystalline groundmass. Plagioclase laths are set in altered groundmass which forms sub ophitic textures (Fig. 5a). Plagioclase phenocrysts occur in prismatic laths and anhedral to subhedral grains in a fine-grained groundmass. Albite twinning is frequently observed in plagioclase which is partially to completely altered to sericite (Fig. 5b). The plagioclase grain range in composition from albite to oligoclase and are found as phenocrysts in the fine groundmass. The boundaries of the large plagioclase phenocrysts are more altered than their cores. Some samples contain 4 mm long plagioclase grains (Fig. b). In few samples of the Zbc volcanic rocks the euhedral to anhedral grains of the pyroxene and olivine are pseudomorphed by chlorite, epidote, actinolite and opaque minerals (Fig. 5c, d). Clinopyroxene is represented by augite which is partially to completely altered to chlorite. A few larger grains of augite are embedded in the fine-grained groundmass, are mainly subhedral in shape and form a porphyritic texture (Fig. 5d).

The basalt of Zhm consists of plagioclase, clinopyroxene, orthopyroxene, and minor olivine, opaque and glassy materials (Fig. 5 e-h). Plagioclase occurs as phenocrysts and fine grained ground mass. Plagioclase phenocrysts are subhedral to anhedral in shape with visible albite twining and the rock has a sub-ophitic texture (Fig. 5e and f). Plagioclase is highly altered to sericite in some samples (Fig. 5g). Clinopyroxene is found as phenocrysts and fine-grained groundmass (Fig. 5g, h) and is highly altered to chlorite. Phenocrysts of clinopyroxene are surrounded by fine-grained ground mass made up of plagioclase and pyroxene which shows sub-porphyritic texture (Fig. 5h). The groundmass comprises fine-grained hemi-crystalline plagioclase and clinopyroxene, and opaque materials show aphanitic texture. Secondary minerals: quartz, calcite and zeolites occur as fine-grained aggregate and as amygdales.

4.3. Geochemistry

4.3.1. Basalt Chert Unit Lavas of the Zhob Ophiolite

Seven basaltic rock samples of this unit (one from the Ali Khanzai block, four from the Naweoba block and two from the Omzha block) of the Zhob Ophiolite were analyzed for geochemistry. The major oxides from Zbc range from; SiO_2 = 45.34 – 75.22 wt. %; Al_2O_3 = 6 – 15.45 wt. %; TiO_2 = 0.3 – 1 wt. %; Fe_2O_3 = 2.51 – 9.61 wt. %; K_2O = 0.01 – 1.77 wt. %; P_2O_5 = 0.02 – 0.08 wt. %; MgO = 1.74 – 12.14 wt. %; CaO = 3.76 – 19.57 wt. %; Na_2O = 0.30 – 5.36 wt. %. (Table. 1).

The total alkali versus silica (TAS) diagram of (Le Bas et al. 1986), was used to classify the rocks. The Naweoba block samples plot in basalt field, trachy-basalt, basalt andesite and in the dacite field. The Ali Khanzai block rocks plot in the dacite field while the two samples of the Omzha block plot in the basalt field (Fig. 8a). The basaltic rock samples from the Zbc of Zhob ophiolite have also been plotted on an immobile trace element Co versus Th classification diagram for altered volcanic rocks (Fig. 8b; after Hastie et al. 2007) which fall in basalt field.

The basaltic rocks of this unit of tholeiite nature with high Al_2O_3 (6 – 15.45 wt. %), low MgO (1.74 – 12.14 wt. %), TiO_2 (0.29 – 1 wt. %) and K_2O (0.01 – 1.77 wt. %) that resemble the MORB type. The basaltic rocks of the Zbc of the Zhob Ophiolite are extensively altered and the samples were plotted on Zr/Ti versus Nb/Y diagram of (Pearce 1996) which is resistant to the effects of alteration. This diagram confirms the basaltic nature all the Zbc rock samples (Fig. 9a).

MgO and Zr of volcanic rocks on the Harker diagram were plotted against other major and trace elements which show clear fractionation trends (Fig. 6, 7). To determine the nature of volcanic rocks of Zbc they have been plotted on the Zr versus P_2O_5 diagram (Winchester and Floyd 1976), which confirms that these rocks are tholeiitic in nature (Fig. 9b). These volcanic rocks were also plotted on Nb/Y versus Ti/Y diagram (Fig. 9c), (Pearce 1982) that show their tholeiitic nature. The triangular $MnO/TiO_2/P_2O_5$ diagram (Mullen 1983), (Fig. 9d) further confirms the tholeiitic nature of the basaltic rocks of the Zbc of the Zhob Ophiolite and this diagram also suggests that these volcanic rocks have an island arc tholeiite signature. The Ti/V ratio of basaltic rocks of the Zbc ranges from 13 – 60 (Fig. 9f) and plot in the MORB and arc tholeiite field on the Ti vs. V diagram.

These diagrams confirm characteristics which are intermediate between NMORB and IAT (Fig. 9e), (after Pearce et al. 1981). Therefore, it is likely that due to modification of the depleted mantle by a subducted slab component these basaltic rocks were formed in an oceanic environment in a manner similar to that proposed for the lavas of Bagh complex in Early Cretaceous during the break up of Gondwanaland (Kojima et al. 1994). The geochemical features of the basaltic rocks of Zbc are typical of arc tholeiite that formed in back-arc basins (Fig. 9f; Dilek and Furnes 2011), which suggest a supra-subduction zone tectonic setting.

On an N-MORB normalized plot, the high field strength (HFS) elements such as (Zr, Ti, Y, and Sm) show a flat pattern parallel to N-MORB (Sun and McDonough 1989). The large ion lithophile (LIL) elements such as (Gd, Dy, Ho, and Lu) show more enrichment than N-MORB (Fig. 10a), but this is most likely due to LIL element enrichment during alteration. The enrichment of Th and depletion of Nb compared to other immobile elements indicate a subduction zone component (Wood 1980). On chondrite-normalized REE diagrams these rocks have depleted LREE and flat HREE patterns typical of NMORB (Fig. 10c).

4.3.2. Hyaloclastite-Mudstone Unit Lavas of the Zhob Ophiolite

Five basaltic rock samples of the hyaloclastite mudstone unit (three from the Ali Khanzai block, one from the Naweoba block and one from the Omzha block) of the Zhob Ophiolite were analyzed for geochemistry. The major oxides of the basaltic rocks of the hyaloclastite mudstone unit of all three blocks of the Zhob Ophiolite are; SiO_2 = 39.35 – 44.99 wt. %; TiO_2 = 2.02 – 3.95 wt. %; Al_2O_3 = 11.80 – 14.83 wt. %; Fe_2O_3 = 6.21 – 14.22 wt. %; MgO = 2.36 – 9.44 wt. %; CaO = 9.65 – 15.78 wt. %; Na_2O = 2.00 – 4.34 wt. %; K_2O = 0.03 – 3.32 wt. %; P_2O_5 = 0.39 – .79 wt. %. (Table. 1). The volcanic rocks of the Zhm are of an alkaline nature with low Al_2O_3 and high TiO_2 and MgO of OIB type rocks.

The total alkali versus silica (TAS) diagram of (Le Bas et al. 1986) was used to classify the rocks. The one sample from the Naweoba block plots in the foidite field, three samples of Ali Khanzai block plot in the tephrite basanite field while the one sample from Omzha block plots in the picro-basalt field (Fig. 8a). Due to rock alteration and to check the remobilization of alkalis the hyaloclastite-mudstone unit was also plotted on several immobile element classification diagrams. On the Co versus Th classification plot (Fig. 8b), (after Hastie et al. 2007) the lavas of this unit plot in the basaltic field and on the Zr/Ti versus Nb/Y diagram of (Pearce 1996) the samples classified as alkali basalt field (Fig. 9a).

Mg and Zr of volcanic rocks on the Harker diagram were plotted against other elements that show well-defined fractionation trends and these volcanic rocks are likely to have been fractionated in upper-level magma chamber and are not directly derived from the partial melts from a mantle source (Figs. 6, 7).

Since the HFS elements are least altered by secondary alteration they can be used for determining the tectonic setting of these rocks. The P_2O_5 versus Zr diagram (Winchester and Floyd 1976) and the Ti/Y versus Nb/Y diagram (Pearce 1982) confirm that these rocks are alkaline in nature (Fig. 9b, c). The $MnO/TiO_2/P_2O_5$ triangular diagram (Fig. 9d; after Mullen 1983), the basalts of the hyaloclastite mudstone unit suggest that these volcanic rocks were formed by hot spot derived magmatism. This is confirmed by the Zr versus Ti diagram (Pearce et al. 1981), which also indicates that these rocks have geochemical characteristics of within plate lavas (Fig. 9e). Finally, the Ti versus V diagram confirms that these alkaline rocks were formed in the ocean island tectonic setting (Fig. 9f; Dilek and Furness 2011),

On N-MORB and chondrite normalized diagrams (Sun and McDonough 1989) some high field strength (HFS) elements show depletion while the large ion lithophile (LIL) elements show enrichment (Fig. 10b). However, the enrichment in LIL elements may well be due to element mobility caused by hydrothermal alteration. On chondrite-normalized REE plots the hyaloclastite mudstone unit rocks are depleted in HREE compared to N-MORB (Fig. 10d). Both N-MORB and chondrite normalized diagrams show that these rocks have similar patterns to those of OIB type magmatic rocks.

5. Discussion

The Zhob ophiolite is part of Zhob valley ophiolites, is highly deformed and dismembered and thrusted onto the passive continental margin sediments of Indian plate (Jones 1961). It is unconformably overlain by early Eocene sediments Pishin flysch zone (Kasi et al. 2012). The Zhob ophiolite comprises three detached ophiolitic blocks; Ali Khanzai block, Omzha block, and Naweoba block. These blocks of the Zhob ophiolite consists of various units of sedimentary, igneous and metamorphic rocks. These mapped units are mostly fault-bounded with one another. They are, crustal plutonic rock unit (*Zcp*), Mantle section rocks unit (*Zms*), Metamorphic rocks (*Zmr*), Basalt chert rock unit (*Zbc*), Hyaloclastite mudstone rock unit (*Zhm*) and Lower and upper sedimentary rock unit (*Zls & Zus*). Basalt Chert unit (*Zbc*) covers about 60% area of Ali Khanzai, 50% of Omzha and 40% of the Naweoba blocks (Fig. 2). The Zbc unit is composed of thick pillow lava associated with red chert, pelagic and hemipelagic limestone and mudstone and hyaloclastite. Hyaloclastite Mudstone unit (*Zhm)* covers about 50% of the area of Naweoba, 40% of Ali Khanzai and 30% of the Omzha block (Fig. 2a, b, c). The basalt chert unit (Zbc), is composed of thick pillow lava associated with bedded chert, pelagic limestone, hyaloclastite and hemi-pelagic mudstone. The hyaloclastite mudstone (Zhm), is comprised of basaltic rocks with limestone, hemipelagic siliceous mudstone, shale, and occasionally tuff and fragments of volcanic, ultramafic, mafic and sedimentary rocks were also observed. These rock units of Zhob Ophiolite were deposited on the Indian continental slope to the ocean floor of the Ceno-Tethys branch (Naka et al. 1996).

5.1. Petrogenesis of Zhob Lavas

Geochemical composition of volcanic rocks of ophiolite are important in assessing, petrogenesis, magmatic evolution and tectonic setting of ophiolite complexes (Pearce and Cann 1973; Pearce et al. 1984). The high field strength elements (HFSE), REEs and some Transitional elements (such as Ti, V) are considered to be immobile during hydrothermal alteration of ocean floor and metamorphism (Pearce 2014). Conversely, certain major (Si, Na, K, Ca) and trace (Cs, Rb, Ba, Sr) elements may be modified during hydrothermal seafloor alteration and/or metamorphism (Gillis 1995; Gillis and Banerjee 2000). The geochemical studies reveal that the Naweoba block volcanic rocks of the Zbc unit plot in the basalt field, trachy-basalt, basalt andesite and in the dacite field (Fig. 8a). The Ali Khanzai block sample plots in the dacite field while the two samples of Omzha block fall in the basalt field. The Naweoba block volcanic rocks sample of Zhm unit plots in the foidite field, the three samples of the Ali Khanzai block plot in the tephrite basanite field while the one sample from Omzha block plots in the picro-basalt field with alkaline in nature, by plotting on the (TAS) Diagram (Fig. 8a). The basaltic rocks of basalt chert unit of tholeiite nature have a major oxide chemistry with high Al_2O_3 (5.98 – 15.45 wt. %), low MgO (1.74 – 12.14 wt. %), TiO_2 (0.29 – 0.98 wt. %) and K_2O (0.01 – 1.77 wt. %). Generally, low contents of TiO_2 (less than 1 wt. %) in basaltic rocks are attributed to subduction processes. Major oxide concentrations in volcanics rocks of the basalt chert unit of Zhob Ophiolite are similar to tholeiitic basalts of Chaldoran massif Iran (Moharami et al. 2014) and resemble MORB type. The basaltic rocks of Zhm are of alkaline nature with low Al_2O_3 (11.80 -14.83 wt. %), high TiO_2 (2.02 – 3.95 wt. %), MgO (2.36 – 9.44 wt. %) and K_2O (0.03 – 3.32 wt. %). They are similar in composition to the alkaline Chaldoran volcanoclastic rocks in Iran (Moharami et al. 2014) and resemble OIB type.

All three ophiolitic bodies of Zhob Ophiolite containing tholeiitic, N-MORB like basalt from Zbc unit and alkali basalt of OIB type from the Zhm unit. The (HFS) elements such as (Zr, P, Y, Ti, and Sm) show a flat pattern parallel to N-MORB on an N-MORB normalized plot (Sun and McDonough 1989) while the (LIL) elements such as (Gd, Dy, Ho, and Lu) shows enrichment than N-MORB of the basaltic rocks of the Zbc unit (Fig. 10a, c). This enrichment of LIL elements can be due to mobilization of elements during metasomatism or modification of the depleted mantle by a subducted slab component. The enrichment of Th and depletion of Nb compared to other immobile elements is a distinctive characteristic and indicate a subduction zone component (Wood 1980; Aydin et al. 2008). Such characteristics are observed in the tholeiitic basalts of other ophiolites of supra-subduction origins like Neyriz Ophiolite (Iran), Chaldoran massif (Iran), (Moghadam et al. 2014; Moharami et al. 2014). On chondrite normalized diagrams these rocks display REE patterns with depletion in most of LREE and they have a flat HREE pattern typical of NMORB and are similar to supra subduction zone basaltic rocks of the Cicekdag Ophiolite (Turkey; Yaliniz et al. 2000)

The basaltic rocks of the hyaloclastite mudstone unit on N-MORB and chondrite normalized diagrams (Fig. 10b, d) (Sun and McDonough 1989) some (HFS) elements show depletion while (LIL) elements show enrichment which is similar to intraplate continental basalts. Depletion and enrichment in HFS and LIL elements, respectively, are identical to the OIB basalts from Armenian Ophiolite and Ankara Mélange (Rolland et al. 2009; Bortolotti et al. 2018). The hyaloclastite mudstone unit rocks on chondrite normalized REE plots shows depletion in the HREE compared to N-MORB. Both N-MORB and chondrite normalized diagrams indicate that these rocks have similar patterns to those of OIB type.

The Ti/Y versus Nb/Y diagram and Zr versus Ti diagram, (Pearce et al. 1981) differentiate among MORB, WPB and VAB. The basaltic rocks from the Zbc fall in MORB and VAB while volcanic rocks of Zhm fall in the WPB field. The volcanic rocks of Zbc and Zhm also plot on a V versus Ti diagram (Fig. 9f; Dilek and Furnes 2011) that the basaltic chert unit rocks plot in the overlapping field of N-MORB and IAT while the Zhm falls in the WPB field. Such characteristics of basalt of hyaloclastite mudstone units are comparable to the within-plate OIB basalt of Ankara Mélange (Bortolotti et al. 2018).

5.2. Comparison of Zhob Lava with Muslim Bagh and Waziristan ophiolites' Lava.

In the following section, the field relations and geochemistry of the Zhob lavas will be compared with that of Muslim Bagh ophiolite (South) and Waziristan ophiolite (North). The Waziristan ophiolite is dismembered and separated into three nappes, such as The Vezhda Sar nappe, which is consists of pillow type basalts and hyaloclastite, the Boya nappe with intact ophiolite section which is a tectonic mélange and the Datta Khel nappe, that comprises dykes and with other components (Khan 2000). To the west, the Waziristan ophiolite nappes are unconformably overlain by Early to Middle Eocene age sedimentary rocks which supports the Paleocene emplacement. To the east, the Waziristan ophiolite units have been thrust over the passive continental margin sedimentary rocks of the Indian plate (Khan et al. 2007).

The1Muslim Bagh1ophiolites are well-exposed ophiolites in Pakistan. This ophiolite is divided into four zones: the flysch zone, the Muslim Bagh ophiolite, the Bagh complex, and the passive margin. The Muslim Bagh ophiolite1comprises of two massifs; the Jang1Tor Ghar Massif (JTGM) in the west and the Saplai Tor Ghar1Massif (STGM) in the east (Bilgrami 1964). The Bagh complex consists of a serpentine matrix mélange unit, ultramafic and mafic unit, hyaloclastite mudstone unit, basalt chert unit and sedimentary rock unit (Mengal et al. 1994, Siddiqui et al. 1996, Kakar et al. 2012).

Similar basaltic rocks are reported from all the three Tethyan ophiolite complexes (Muslim Bagh, Zhob, and Waziristan). The Bagh complex, consists of two main units named the hyaloclastite mudstone unit (Bhm) which is alkaline in nature and the basalt chert unit (Bbc) which is tholeiitic in nature (Kakar et al. 2012). The Bbc unit is composed of thick pillow lava associated with red chert, pelagic and hemipelagic limestone and mudstone while the Bhm unit comprises basaltic rocks with limestone and siliceous mudstone (Siddiqui et al. 1996; Kakar et al. 2012). The volcanic rocks of the same characteristics are reported from the Waziristan Ophiolite (Khan 2000) and as has been shown above are present in all three ophiolitic bodies of the Zhob ophiolite. The lithology, age and structural similarities of the basaltic rocks of the Bagh complex are similar in the Waziristan, Zhob and Bela ophiolites (Siddiqui et al. 1996; Kakar et al. 2012; Khan et al. 2007). These volcanic rocks range in age from Early-Late Cretaceous (Kojama et al. 1994). The basaltic rocks of the Bbc unit have been interpreted as the Neo-Tethyan ocean floor that was formed during the breakup of Gondwana (Kakar et al. 2012) Conversely, the alkali basaltic rocks of the Bhm unit were formed by the melting of an OIB-type (hotspot-derived) source region during the Middle-Late Cretaceous (Kojama et al. 1994; Kakar et al. 2012).

Volcanic and volcanoclastic Zhob ophiolite rocks exhibit similar geochemical characteristics to the Muslim Bagh, and Waziristan ophiolites (Fig. 9, 10) and all three ophiolites have geochemical signatures of a supra-subduction zone tectonic setting that formed in the Neo-Tethys Ocean (80-70 Ma) and was then obducted on the Indian passive continental margin sediments between 70-65 Ma (Kakar et al. 2012). The Muslim Bagh, Zhob and Waziristan ophiolites are transitional between an island arc and mid-oceanic ridges setting which suggests a supra subduction zone origin.

Shortly, the basaltic rocks of the basalt chert unit of Zhob Ophiolite represent the Neo-Tethyan ocean floor that was formed during the breakup of Gondwana. The alkaline volcanic rocks of the hyaloclastite mudstone unit have been formed by the melting of an intra-plate (possibly hotspot-derived) source region during the Middle-Late Cretaceous. On N-MORB normalized diagrams both the Zbc lava and Zhm lava of all three ophiolitic blocks of the Zhob ophiolite show negative Nb and Ta anomalies indicating that these rocks contain either a subduction component or continental crust. The depletion of Nb and Ta anomalies of the shallow derived MORB like the lava of Zbc and the deep mantle plume derived OIB like the lava of the Zhm describe the subduction process. However, during the breakup of the Gondwana, significant fragments of continental crust may have been incorporated into the Tethyan ocean basin. The tholeiitic rocks of the Zbc suggest supra subduction zone setting while the Zhm suggests OIB tectonic setting.

6. Conclusions

The Zhob Ophiolite consists of three fault-bounded ophiolitic blocks, known as Ali Khanzai block, Omzha block and Naweoba block. These three ophiolitic blocks consist of various units of sedimentary, igneous and metamorphic rocks such as: Crustal plutonic rock unit (*Zcp*), Mantle section rocks unit (*Zms*), Metamorphic rocks (*Zmr*), Basalt chert rock unit (*Zbc*), Hyaloclastite mudstone rock unit (*Zhm*) and Lower and upper sedimentary rock unit (*Zls & Zus*). The volcanic rocks of the *(Zbc)* are composed of thick pillow lava associated with red chert, pelagic and hemipelagic limestone and mudstone while the volcanic rocks of the (*Zhm*) comprise of basaltic rocks with limestone and siliceous mudstone. The basaltic rocks of the (*Zbc*) are N-MORB-like oceanic tholeiitic basalt, while those of the (Z*hm*) are OIB-like alkali basalts. The basaltic rocks of the *(Zbc)* may represent the Neo-Tethyan ocean floor that was formed during the breakup of Gondwana. Conversely, the alkali basalts of the hyaloclastite mudstone unit are likely to have formed by the melting of an intraplate (hotspot derived) source region during the Middle-Late

Cretaceous. The negative Nb and Ta anomalies of the shallow derived MORB like the lava of the (*Zbc*) and the intraplate OIB like the lava of the (*Zhm*) indicate that the rocks contain a subduction component.

Acknowledgments

This research was financially supported by Higher Education Commission Pakistan (HEC); 1) HRD Foreign scholarships of the Federal PSDP development project "Capacity Building and Strengthening of the Centre of Excellence in Mineralogy". 2) The Higher Education Commission, Pakistan "National Research Program for Universities (NRPU) Project # 3593" to M. Ishaq Kakar. The authors are thankful to the reviewers for their constructive comments which improved the manuscript.

References

Ahmed A, Kakar MI, Naeem A, Ahmed N, Khan M, Panezai M (2020) Geology and Petrology of Omzha Block, Zhob Ophiolite, northern Balochistan, Pakistan. Pak J Geol 4 (2), 72-80

Ahmed Z (1991) A supra-subduction origin of the Bela Ophiolite indicated by acidic rocks, Khuzdar District, Pakistan. Acta Miner Pak 5: 9-24

Ahmed Z (1993) Leucocratic rocks from the Bela Ophiolite, Khuzdar District, Pakistan. In: Treloar PJ, Searle MP (Eds.), Himalayan Tectonics. Geol Soc Lond Spec Publ 74: 89–100

Aydin F, Karsli O, Chen B (2008) Petrogenesis of Neogene alkaline volcanics with implications for post-collisional lithospheric thinning of the eastern Pontides, NE Turkey. Lithos 104: 249-266

Bilgrami, SA (1964a) Mineralogy and petrology of the central part of the Hindu Bagh igneous complex, Hindubagh Mining District, Zhob Valley, West Pakistan. Geol Surv Recs 10: 28

Bortolotti V, Chiari M, Göncüoglus MC, Principi G, Saccani G, Tekin UK, Tassinari R (2018) The Jurassic–Early Cretaceous basalt–chert association in the ophiolites of the Ankara Mélange, east of Ankara, Turkey: age and geochemistry. Geol Mag 155 (2): 451–478

Dilek Y, Furnes H (2011) Ophiolite genesis and global tectonics: geochemical and tectonic fingerprinting of ancient oceanic lithosphere. Geol Soc Am Bull 123: 387–411

Gansser A (1979) Reconnaissance visits to the ophiolites in Balochistan and the Himalaya. In: Farah A, DeJong KA (Eds) Geodynamics of Pakistan. Geol Surv Pak 206-209

Gillis KM (1995) Controls on hydrothermal alteration in a section of fast-spreading oceanic crust. Earth and Planet Sci Lett 134: 473–489

Gillis KM, Banerjee NR (2000) Hydrothermal alteration patterns in supra-subduction zone ophiolites. In: Dilek Y, Moores EM (Eds) Ophiolites and Oceanic Crust: New Insights from Field Studies and Ocean Drilling Program, 283–297

Dilek Y, Furnes H (2014) Ophiolites and their origins. Elements 10: 93–100

Hastie AR, Kerr AC, Pearce JA, Mitchell SF (2007) Classification of altered volcanic island arc rocks using immobile trace elements: development of the Co–Th discrimination diagram. J Petrol 48: 2341–2357

Iqbal M, Shah M I (1980) A guide to the stratigraphy of Pakistan. Rec Geol Surv Pak 53, 34

Jones (1961) Reconnaissance Geology of part of West Pakistan, a Columbo Plan cooperative project. Hunting Survey Corporation, Government of Canada, Toronto

Kakar MI, Collins AS, Mahmood K, Foden JD, Khan M (2012) U–Pb Zircon crystallization age of the Muslim Bagh Ophiolite: enigmatic remains of an extensive pre-Himalayan arc. Geology 40 (12): 1099–1102

Kakar MI, Kerr AC, Mahmood K, Collins AS, Khan M, McDonald I (2014) Supra-subduction zone tectonic setting of the Muslim Bagh ophiolite, northwestern Pakistan: insights from geochemistry and petrology. Lithos 202-203: 190-206

Kassi AK, Kassi AM, Umar M, Manan RA, Kakar MI (2012) Revised Litho-stratigraphy of the Pishin belt, northwestern Pakistan. J Himalayan Earth Sci 45(1): 53-65

Khan SR (2000) Petrology and geochemistry of a part of Waziristan Ophiolite, NW Pakistan. Unpublished PhD thesis, University of Peshawar 253-255

Khan SR, Jan MQ, Khan MA, Khan T (2001) Geochemistry and petrogenesis of the sheeted dykes from Waziristan Ophiolite, NW Pakistan and their tectonic implications. Abstract: 16th HKT Workshop, Graz, Austria, April 5–8, 2001. J Asian Earth Sci 19(3A), 36

Khan M, Kerr AC, Mahmood K (2007) Formation and tectonic evolution of the Cretaceous–Jurassic Muslim Bagh ophiolitic complex, Pakistan: implications for the composite tectonic setting of ophiolites. J Asian Earth Sci 31: 112–127

Khan MA, Kakar MI, Ulrich T, Ali L, Kerr AC, Mahmood K, Siddiqui RH (2020). Geniuses of Manganese Deposits in the Ali khanzai block of Zhob Ophiolite, Pakistan: Inferences from Geochemistry and Mineralogy. J Earth Sci 31(5): 884-895

Khan MA (2020) Genesis of Economic Minerals from Zhob Valley Ophiolites. PhD Thesis (unpublished), Centre of Excellence in Mineralogy, University of Balochistan, Quetta, Pakistan.

Kojima S, Naka T, Kimura K, Mengal JM, Siddiqui RH, Bakht MS (1994) Mesozoic radiolarians from the Bagh complex in the Muslim Bagh area, Pakistan: their significance in reconstructing the geological history of ophiolites along the Neo-Tethys suture zone. Bull Geol Surv Jpn 45:63–97

LeBas MJ, LeMaitre RW, Streckeisen A, Zanettin B (1986) A chemical classification of volcanic rocks based on the total alkali silica diagram. J Petrol 27: 745-750

Mengal JM, Kimura K, Siddiqui MRH, Kojima S, Naka T, Bakht MS, Kamada K (1994) The lithology and structure of a Mesozoic sedimentary-igneous assemblage beneath the Muslim Bagh Ophiolite, Northern Balochistan, Pakistan. Bull Geol Surv Japan 45: 51–61

Moghadam HS, Stern RJ, Rahgoshay M (2014) The Dehshir ophiolite (central Iran): Geochemical constraints on the origin and evolution of the Inner Zagros ophiolite belt. Geol Soc Am Bull 122(9):1516-1547. DOI: 10.1130/B30066.1

Moharami F, Azadi I, Mir mohammadi M, Ghazi M J, Rahgoshay M (2014) Petrological and geodynamical constrains of Chaloderan basaltic rocks, NW Iran: evidence from geochemical characteristics. Iranian J Earth Sci 6: 31-43

Mullen, Ellen D (1983) a minor element discriminant for basaltic rocks of oceanic environments and its implications for petrogenesis. Earth Planet Sci Lett 62.1: 53-62

Naka T, Kimura K, Mengal JM, Siddiqui RH, Kojima S, Sawada Y (1996) Mesozoic sedimentary-igneous Complex, Bagh Complex, in the Muslim Bagh Area, Pakistan. Opening and closing ages of the Ceno-Tethyan Branch. In Yajima J, Siddiqui RH (Eds) Proceedings of Geoscience Colloquium, Geoscience Laboratory, Geol Surv Pak, Islamabad 16: 47–94

Pearce JA, Cann JR (1973) Tectonic setting of basic volcanic rocks determined using trace element analyses. Earth Planet Sci Lett 19: 290–300

Pearce JA, Alabaster T, Scheton AW, Searle MP (1981) The Oman ophiolite as a Cretaceous arc-basin complex: evidence and implications: Philosophical Transactions Royal Society of London, 299-317

Pearce JA (1982) Trace element characteristics of lavas from destructive plate margins. In Thorpe RS (Eds) Andesite Orogenic Andesite and Related Rocks. Wiley, 525–548

Pearce JA, Lippard SS, Roberts S (1984) Characteristics and tectonic significance of supra-subduction zone ophiolites. In: Kokelaar BP, Howells MF (Eds) Marginal Basin Geology. Volcanic and Associated Sedimentary and Tectonic Processes in Modern and Ancient Marginal Basins: Geol Soc Lond 16: 77–94

Pearce JA (1996) A user's guide to basalt discrimination diagrams. In: Bailes AH, Christiansen EH, Galley AG, Jenner GA, Keith Jeffrey D, Kerrich R, Lentz David R, Lesher CM, Lucas Stephen B, Ludden JN, Pearce JA, Peloquin SA, Stern RA, Stone WE, Syme EC, Swinden HS, Wyman DA (Eds) Trace element geochemistry of volcanic rocks; applications for massive sulphides exploration, Short Course Notes, Geol. Assoc. Canada 12: 79–113

Pearce JA (2003) Supra-subduction zone ophiolites: the search for modern analogues. In: Dilek Y, Newcomb S (Eds) Ophiolite Concept and the Evolution of Geological Thought: Geol Soc Am Bull 373: 269–293

Pearce JA (2014) Immobile element fingerprinting of ophiolites. Elements 10(2):101–108

Rolland Y, Galoyan G, Bosch D, Sosson, Michel M, Fornari, Verati C (2009) Jurassic back-arc and Cretaceous hot-spot series in the Armenian ophiolites — Implications for the obduction process Lithos 112: 163–187

Shervais JW (2001) Birth, death, and resurrection; the life cycle of supra-subduction zone ophiolites. Geochem Geophys 2: 45 (2000GC000080)

Siddiqui RH., Qureshi AA, Mengal JM, Hoshino K, Sawada Y, Nabi G (1994) Petrology and mineral chemistry of Muslim Bagh Ophiolite Complex and its tectonic implications. Proc. Geosc. Coli 9: 17-50

Siddiqui RH, Aziz A, Mengal JM, Hoshino K, Sawada Y (1996) Geology, petrochemistry and tectonic evolution of Muslim Bagh ophiolite complex Balochistan, Pakistan. Geol Geosci Lab Geol Surv Pak 3:11–46

Sun SS, McDonough WF (1989) In: Saunders AD, Norry MJ (Eds) Chemical and isotope systematics of oceanic basalts: implications for mantle composition and processes: Magmatism in the Ocean Basins. Geol Soc Lond Spec Publ. 42: 313–345

Tapponnier P (1981) On the mechanics of the collision between India and Asia. Geol Soc Spec Publ 19: 115–157

Treloar PJ, Izatt CN (1993) Tectonic of the Himalayan collision zone between the Indian plate and the Afghan Blok; a synthesis. In: Treloar PJ and Searle MP (Eds) Himalayan Tectonics. Geol Soc Lond Spec Pub 74: 69-87

Warraich MY, Ali M, Ahmed MN, Siddiqui RH (1995) Geology and structure of the Calcareous zone in the Muslim Bagh in the Qilla Saifullah Area, Balochistan. Geologica, 1: 61-75

Whattam SA, Stern, RJ (2011) The 'subduction initiation rule': a key for linking ophiolites, intra-oceanic fore arcs, and subduction initiation. Contrib Mineral Petrol 162: 1031–1045

Winchester JA, Floyd PA (1976) Geochemical magma type discrimination, application to altered and metamorphosed basic igneous rocks. Earth Planet Sci Lett 28: 459–469

Wood DA (1980) The application of a Th-Hf-Ta diagram to problems of tectono-magmatic classification and to establishing the nature of crustal contamination of basaltic lavas of the British Tertiary volcanic province. Earth Planet Sci Lett 50(1):11–30

Xia L, Li X (2019) Basalt geochemistry as a diagnostic indicator of tectonic setting. Gondwana Res 65: 43–67

Yaliniz K, Göncüoglus MC, Floyd PA (2000) Geochemistry of volcanic rocks from the Cicekdag Ophiolite, Central Anatolia, Turkey, and their inferred tectonic setting within the northern branch of the Neo-Tethyan ocean. In Tectonics and Magmatism in Turkey and the Surrounding Area (Eds E Bozkurt, J Winchester & JA Piper) 203–18. Geol Soc Lond Spec Publ 173

Figures and Table Captions

Fig.1 Geological Map of the Zhob ophiolite and surrounding area, District Zhob, Balochistan Pakistan (modified after Jones 1961).

Fig.2 Geological maps of three ophiolitic blocks of Zhob Ophiolite showing Basalt chert and Hyaloclastite mudstone units with sample locations (a) Naweoba block, (b) Omzha block, (c) Ali Khanzai block.

Fig.3 (a) Very well-developed pillow structures ranging in size from 12 centimeters to 1.5 meters in diameter **(b)** Basalt chert unit is fragmented and makes trusted contact with peridotite, and crustal gabbroic rocks and the doleritic dykes run parallel from north to south in mafic-ultramafic rock units **(c)** The thrusted contact between the ultramafic and mafic rock, basalt chert and hyaloclastite mudstone rock units **(d)** The well exposed amphibolite facies rocks forming high mountain peaks with basalt chert in the Kaza Nalla area of Omzha block.

Fig.4 (a) The sedimentary rock unit is thrusted over the ultramafic and mafic rocks unit while in the north the mafic rocks show thrusted contact with volcanoclastic rocks **(b)** Basalt with amygdaloidal structure filled by secondary minerals such as zeolite, calcite and quartz **(c)** The tuff in the hyaloclastite mudstone unit **(d)** Hyaloclastite with a mix of volcanic, sedimentary and ultramafic to mafic rock fragments.

Fig.5 (a, b) Microphotographs of a thin section of the basalt showing sub ophitic texture in which plagioclase laths are set in groundmass (XPL view 4x10) **(c, d)** Basalt containing plagioclase, clinopyroxene, orthopyroxene and minor olivine with opaque glassy materials (XPL view 4x10) **(e, f)** Albite twinning in plagioclase laths in fine grained groundmass (XPL view 4x10) (4g, h) Phenocrysts of clinopyroxene are surrounded by fine grained groundmass which shows sub-porphyritic texture and plagioclase is highly altered to sericite (XPL view 4x10).

Fig.6 Diagrams of MgO versus selected major and trace elements of the volcanoclastic rocks of the hyaloclastite mudstone unit (red) and volcanic rocks of the basalt chert unit (sky blue) of the Zhob Ophiolite. The analyses from the Muslim Bagh and Waziristan Ophiolites are taken from (Kakar et al. 2014) and (Khan 2000) respectively.

Fig.7 Diagrams of Zr versus selected major and trace elements of the volcanoclastic rocks of the hyaloclastite mudstone unit (red) and volcanic rocks of the basalt chert unit (sky blue) of the Zhob Ophiolite. The analyses from the Muslim Bagh and Waziristan Ophiolites are taken from (Kakar et al. 2014) and (Khan 2000) respectively.

Fig.8 (a) Total alkali versus SiO_2 plot of the volcanic rocks from the basalt chert unit (sky blue in color) and hyaloclastite mudstone unit (red in color) (after Le Bas et al. 1986) **(b)** Classification of altered volcanic rocks of both basalt chert unit (sky blue in color) and hyaloclastite mudstone unit (red in color) using immobile trace elements development of the

Th–Co discrimination diagram (after Hastie et al. 2007). The analyses from the Muslim Bagh and Waziristan Ophiolites are taken from (Kakar et al. 2014) and (Khan 2000) respectively.

Fig.9 (a) Tectonic and classification discrimination diagrams of volcanic rocks (basalt chert unit pink; hyaloclastite rock unit red in colours) on Zr/Ti versus Nb/Y (after Pearce 1996) **(b)** Zr/P_2O_5 versus TiO_2 diagram (after Winchester and. Floyd 1976) **(c)** Nb/Y versus Ti/Y diagram (after Pearce 1982) **(d)** $MnO/TiO_2/P_2O_5$ triangular plot diagram (after Mullen 1983) **(e)** Zr versus Ti diagram (after Pearce et al. 1981) **(f)** Ti versus V diagram (Shervais 1984, Dilek and Furnes 2011). The analyses from the Muslim Bagh and Waziristan Ophiolites are taken from (Kakar et al. 2014) and (Khan 2000) respectively.

Fig.10 (a, b) Multi-element N-MORB normalized diagram of the volcanic rocks from the basalt-chert unit and hyaloclastite mudstone unit. **(c & d)** Chondrite normalized REE diagrams of the volcanic rocks of basalt chert unit the volcanic rocks of Hyaloclastite mudstone unit (after Sun and McDonough 1989). The analyses from the Muslim Bagh Ophiolite is taken from (Kakar et al. 2014) respectively.

Table. 1 Major oxide (wt%), trace and REE elements (ppm) of the volcanic rocks from the Zhob ophiolite (Basalt-Hyalocla). The table data from the Muslim Bagh Ophiolite (*Bbc-*Bhm) and Waziristan Ophiolite (**Basalt-**Hyalocla) are taken from Kakar (2012) and Khan, (2000) respectively.

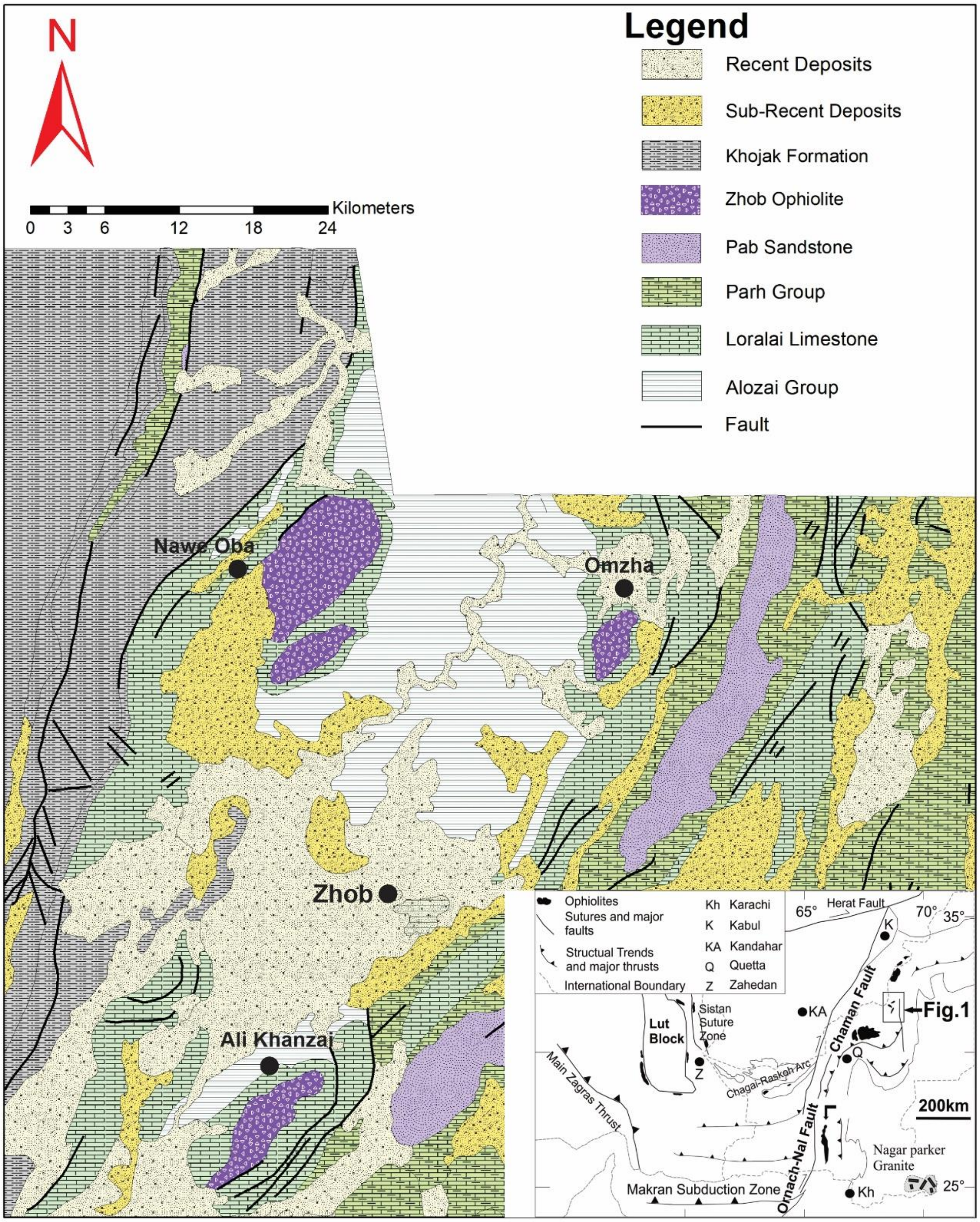

N
Legend
Recent Deposits
Sub-Recent Deposits
Khojak Formation
Zhob Ophiolite
Pab Sandstone
Parh Group
Loralai Limestone
Alozai Group
Fault
0 3 6 12 18 24 Kilometers
Nawe Oba
Omzha
Zhob
Ali Khanzai
Ophiolites
Sutures and major faults
Structual Trends and major thrusts
International Boundary
Kh Karachi
K Kabul
KA Kandahar
Q Quetta
Z Zahedan
65°
Herat Fault
70°
35°
Chaman Fault
Fig.1
Lut Block
Sistan Suture Zone
Chagai-Raskoh Arc
Main Zagras Thrust
200km
Ornach-Nal Fault
Nagar parker Granite
Makran Subduction Zone
25°

Figure 1

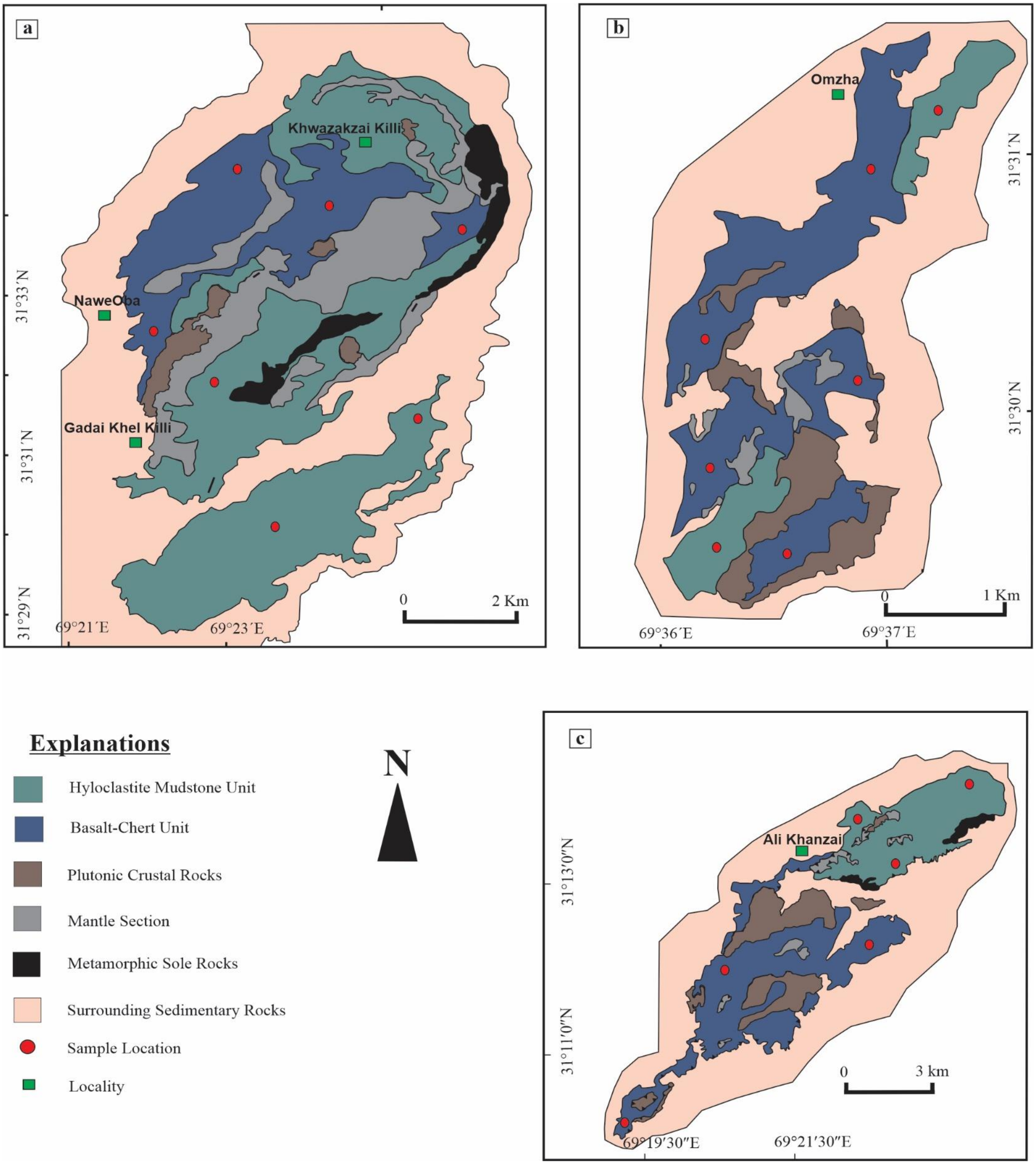

a
Khwazakzai Killi
NaweOba
Gadai Khel Killi
31°33´N
31°31´N
31°29´N
69°21´E
69°23´E
0
2 Km
b
Omzha
31°31´N
31°30´N
69°36´E
69°37´E
0
1 Km
Explanations
Hyloclastite Mudstone Unit
Basalt-Chert Unit
Plutonic Crustal Rocks
Mantle Section
Metamorphic Sole Rocks
Surrounding Sedimentary Rocks
Sample Location
Locality
N
c
Ali Khanzai
31°13′0″N
31°11′0″N
69°19′30″E
69°21′30″E
0
3 km

Fig 2

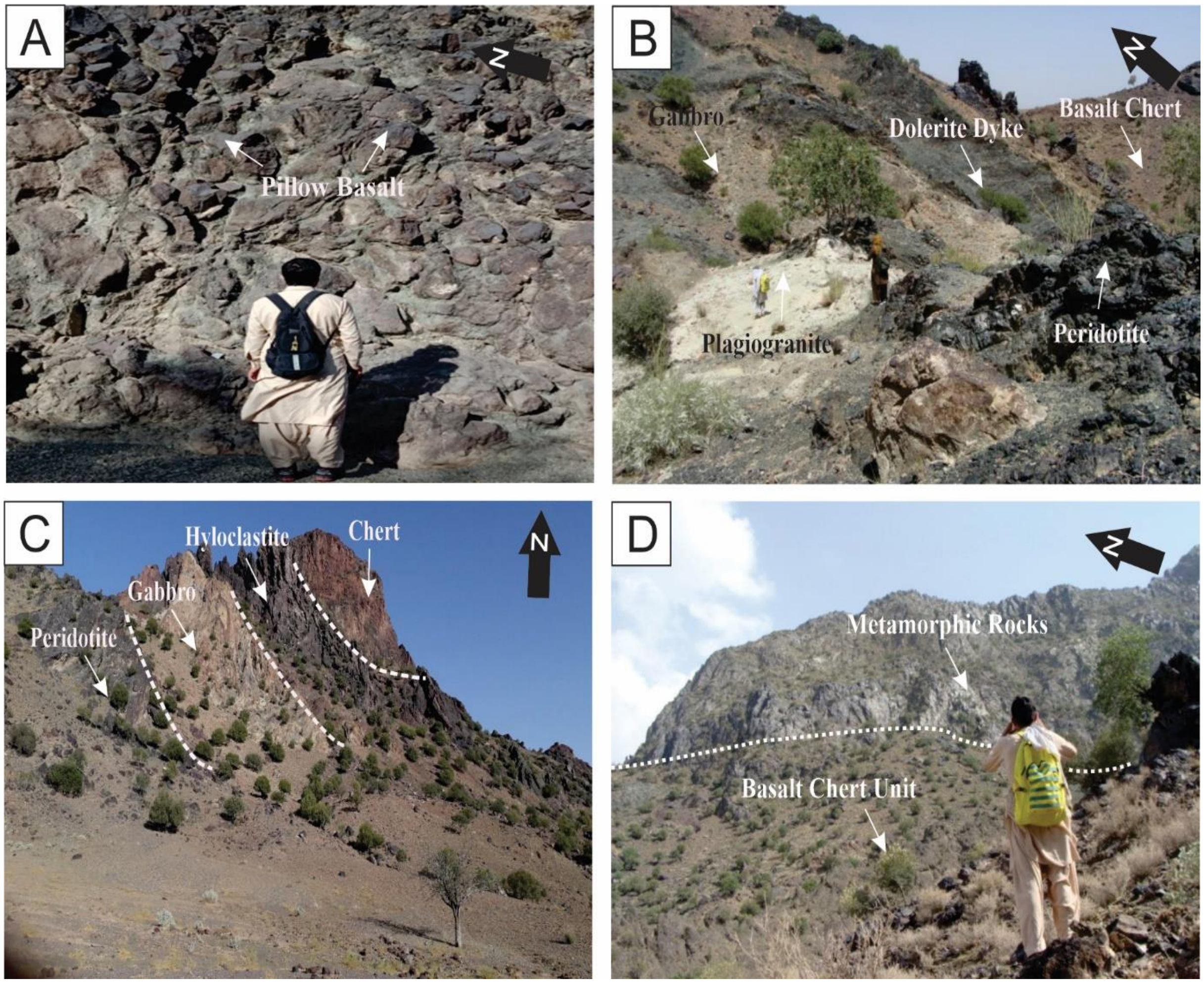
A
Pillow Basalt
B
Gabbro
Dolerite Dyke
Basalt Chert
Plagiogranite
Peridotite
C
N
Hyloclastite
Chert
Gabbro
Peridotite
D
Metamorphic Rocks
Basalt Chert Unit

Figure 3

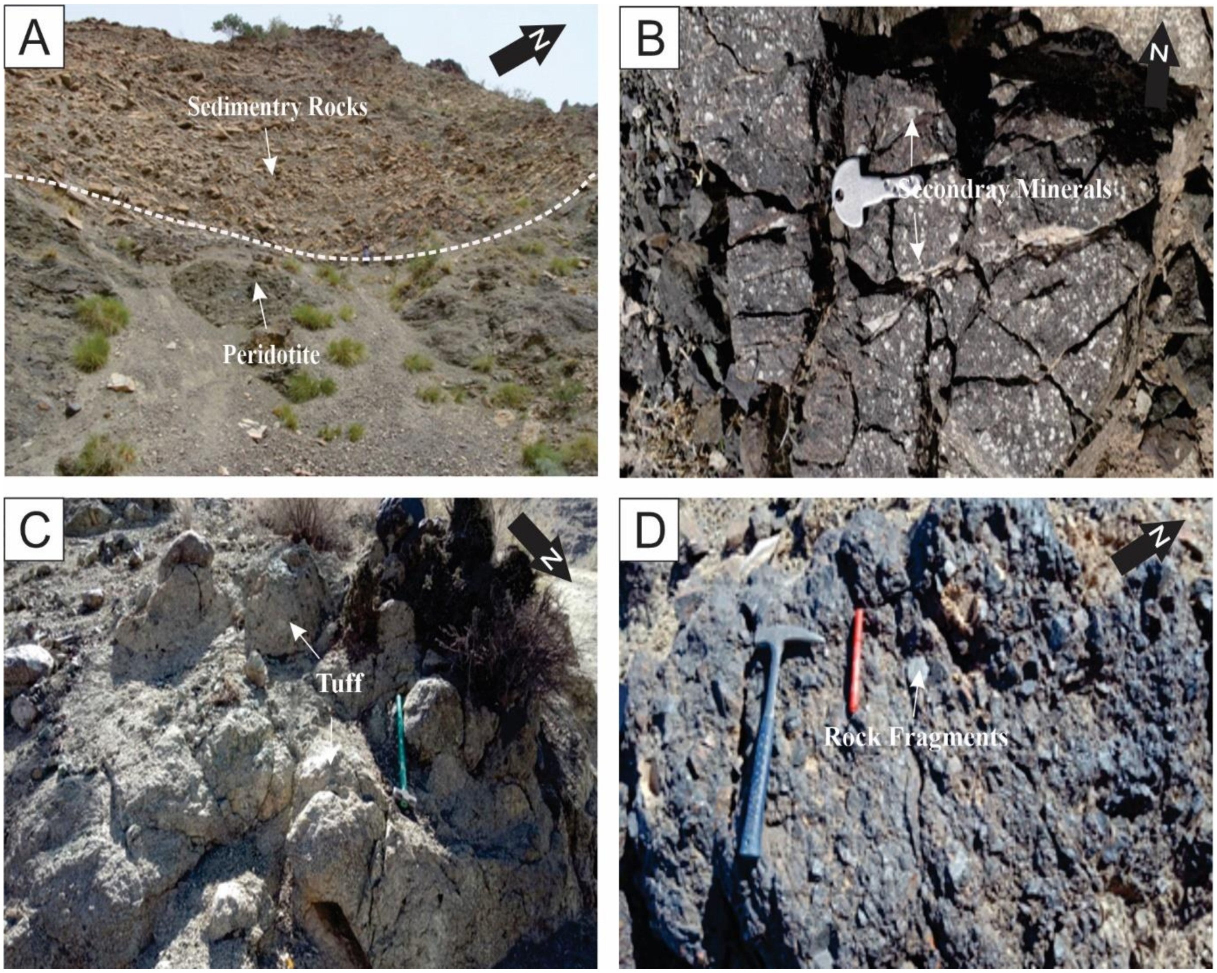
A
N
Sedimentry Rocks
Peridotite
B
N
Secondray Minerals
C
N
Tuff
D
N
Rock Fragments

Figure 4

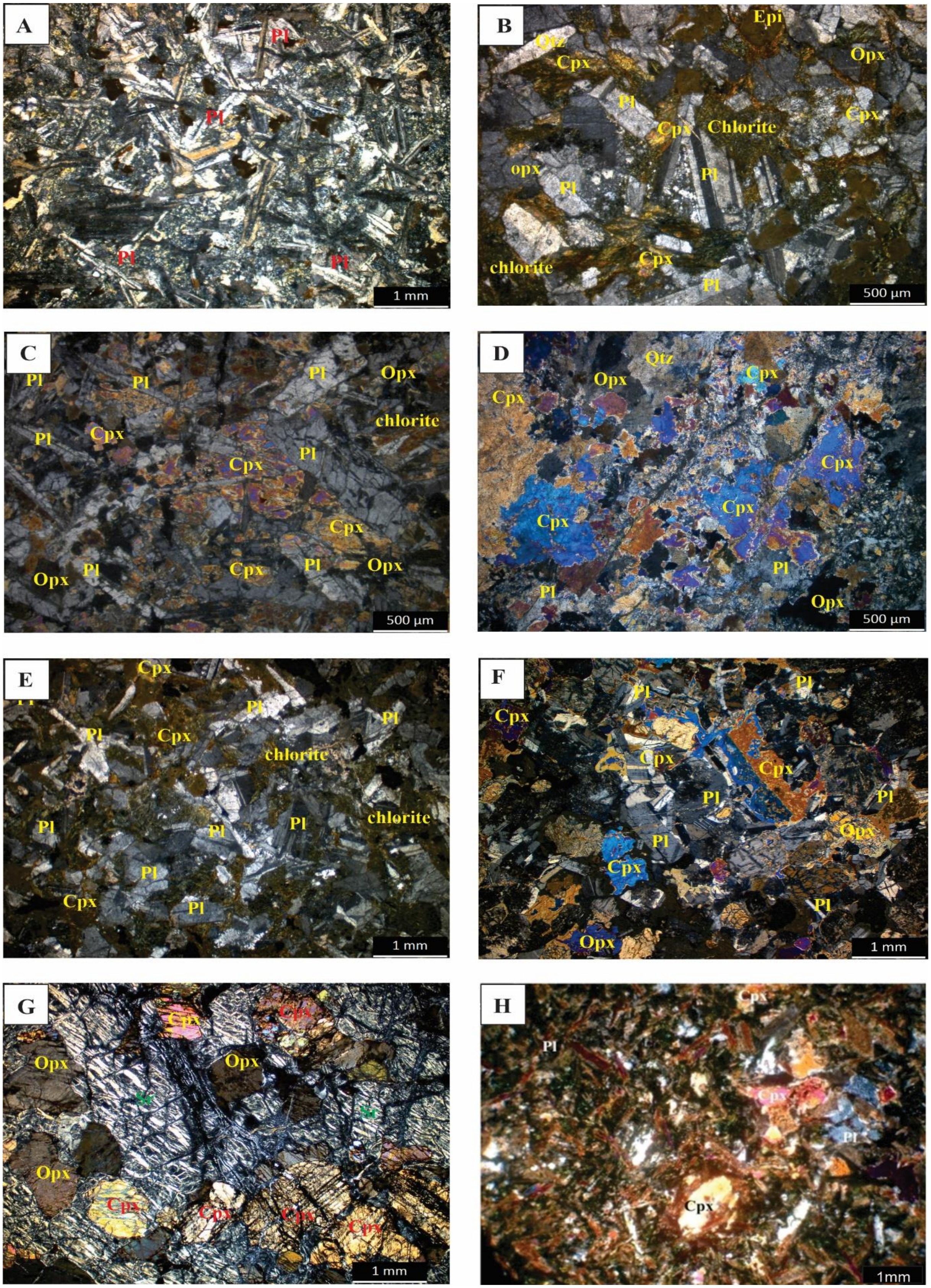
A
Pl
Pl
Pl
Pl
1 mm
B
Epi
Qtz
Cpx
Opx
Pl
Cpx
Chlorite
Cpx
opx
Pl
Pl
chlorite
Cpx
Pl
500 µm
C
Pl
Pl
Pl
Opx
chlorite
Pl
Cpx
Cpx
Pl
Cpx
Opx
Pl
Cpx
Pl
Opx
500 µm
D
Qtz
Opx
Cpx
Cpx
Cpx
Cpx
Cpx
Pl
Pl
Opx
500 µm
E
Cpx
Pl
Pl
Cpx
Pl
chlorite
Pl
Pl
Pl
chlorite
Pl
Cpx
Pl
1 mm
F
Pl
Pl
Cpx
Cpx
Cpx
Pl
Pl
Opx
Pl
Cpx
Pl
Opx
1 mm
G
Cpx
Cpx
Opx
Opx
Opx
Cpx
Cpx
Cpx
Cpx
1 mm
H
Cpx
Pl
Cpx
Pl
Cpx
1mm

Figure 5

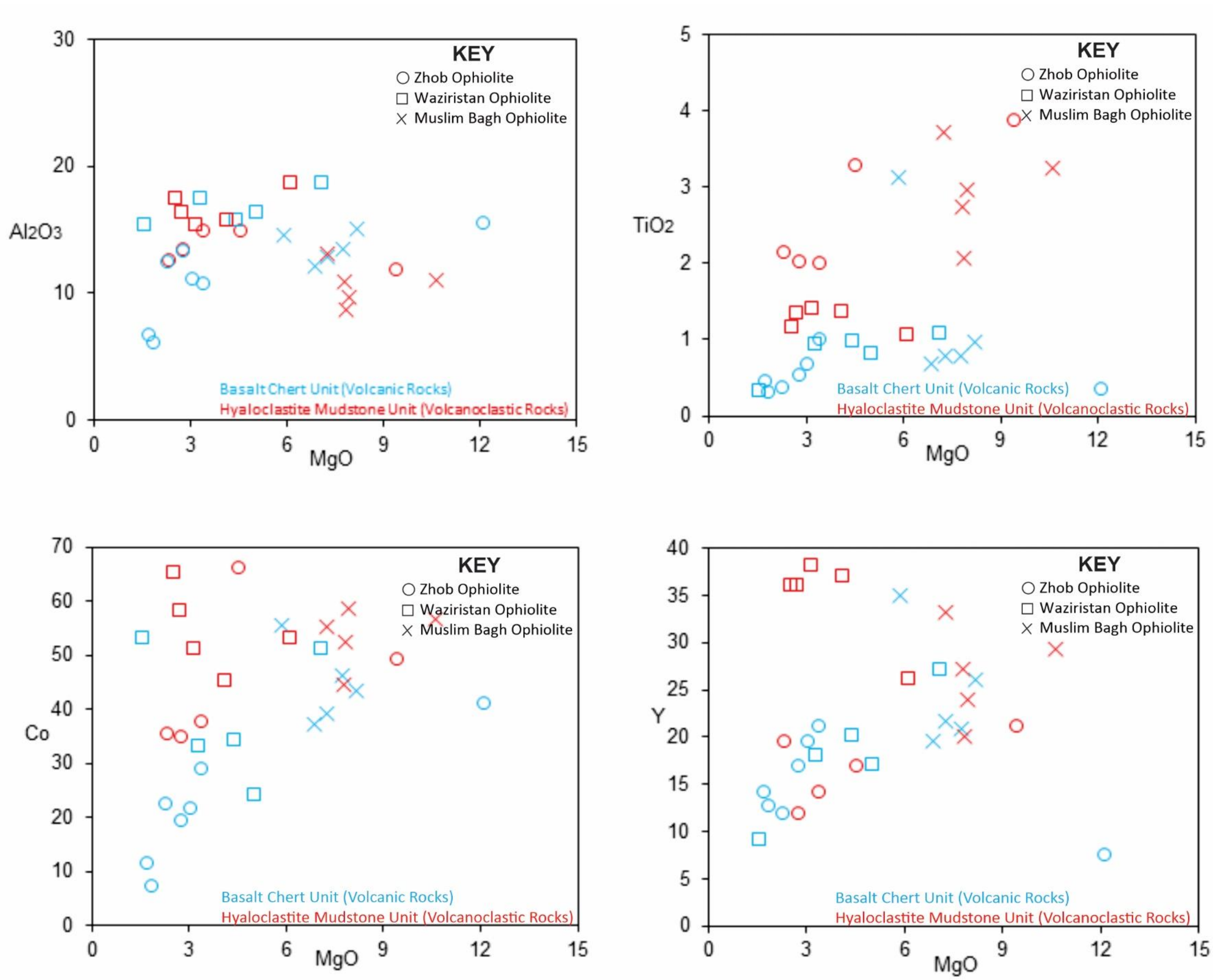
Al2O3
MgO
KEY
Zhob Ophiolite
Waziristan Ophiolite
Muslim Bagh Ophiolite
Basalt Chert Unit (Volcanic Rocks)
Hyaloclastite Mudstone Unit (Volcanoclastic Rocks)
TiO2
MgO
KEY
Zhob Ophiolite
Waziristan Ophiolite
Muslim Bagh Ophiolite
Basalt Chert Unit (Volcanic Rocks)
Hyaloclastite Mudstone Unit (Volcanoclastic Rocks)
Co
MgO
KEY
Zhob Ophiolite
Waziristan Ophiolite
Muslim Bagh Ophiolite
Basalt Chert Unit (Volcanic Rocks)
Hyaloclastite Mudstone Unit (Volcanoclastic Rocks)
Y
MgO
KEY
Zhob Ophiolite
Waziristan Ophiolite
Muslim Bagh Ophiolite
Basalt Chert Unit (Volcanic Rocks)
Hyaloclastite Mudstone Unit (Volcanoclastic Rocks)

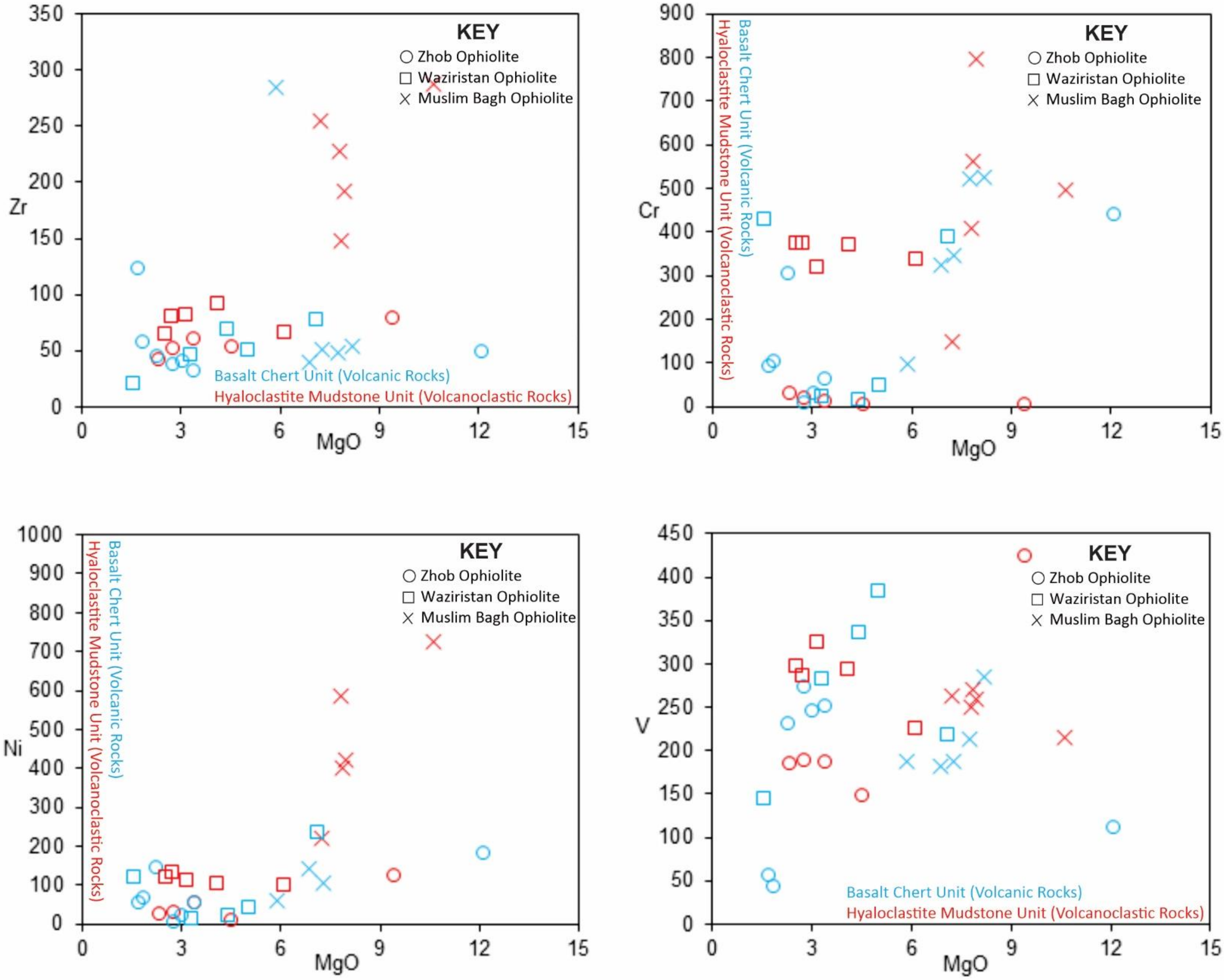

KEY
Zhob Ophiolite
Waziristan Ophiolite
Muslim Bagh Ophiolite
Basalt Chert Unit (Volcanic Rocks)
Hyaloclastite Mudstone Unit (Volcanoclastic Rocks)
Zr
MgO
Cr
Ni
V

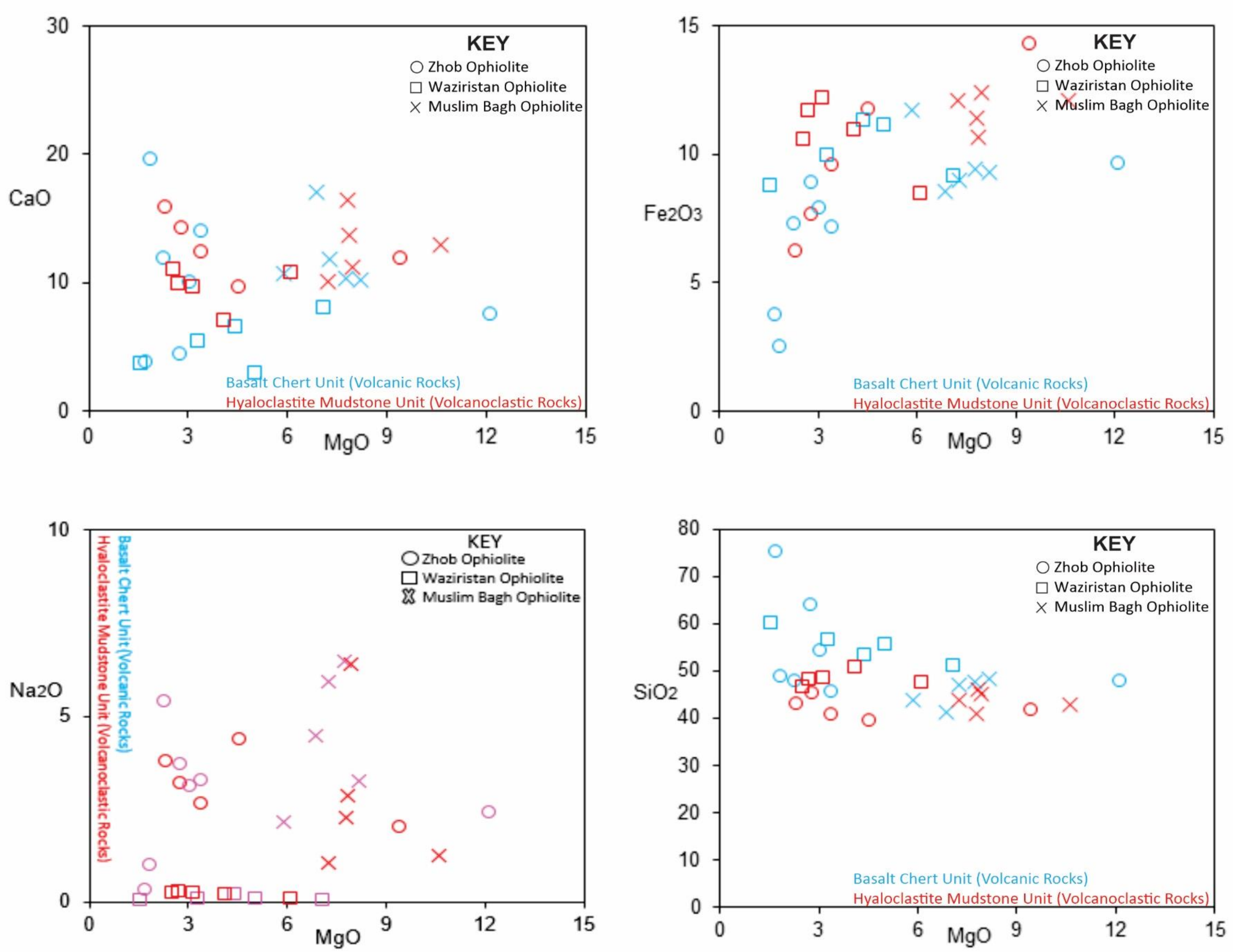

CaO
MgO
KEY
Zhob Ophiolite
Waziristan Ophiolite
Muslim Bagh Ophiolite
Basalt Chert Unit (Volcanic Rocks)
Hyaloclastite Mudstone Unit (Volcanoclastic Rocks)
Fe2O3
Na2O
SiO2

Figure 6

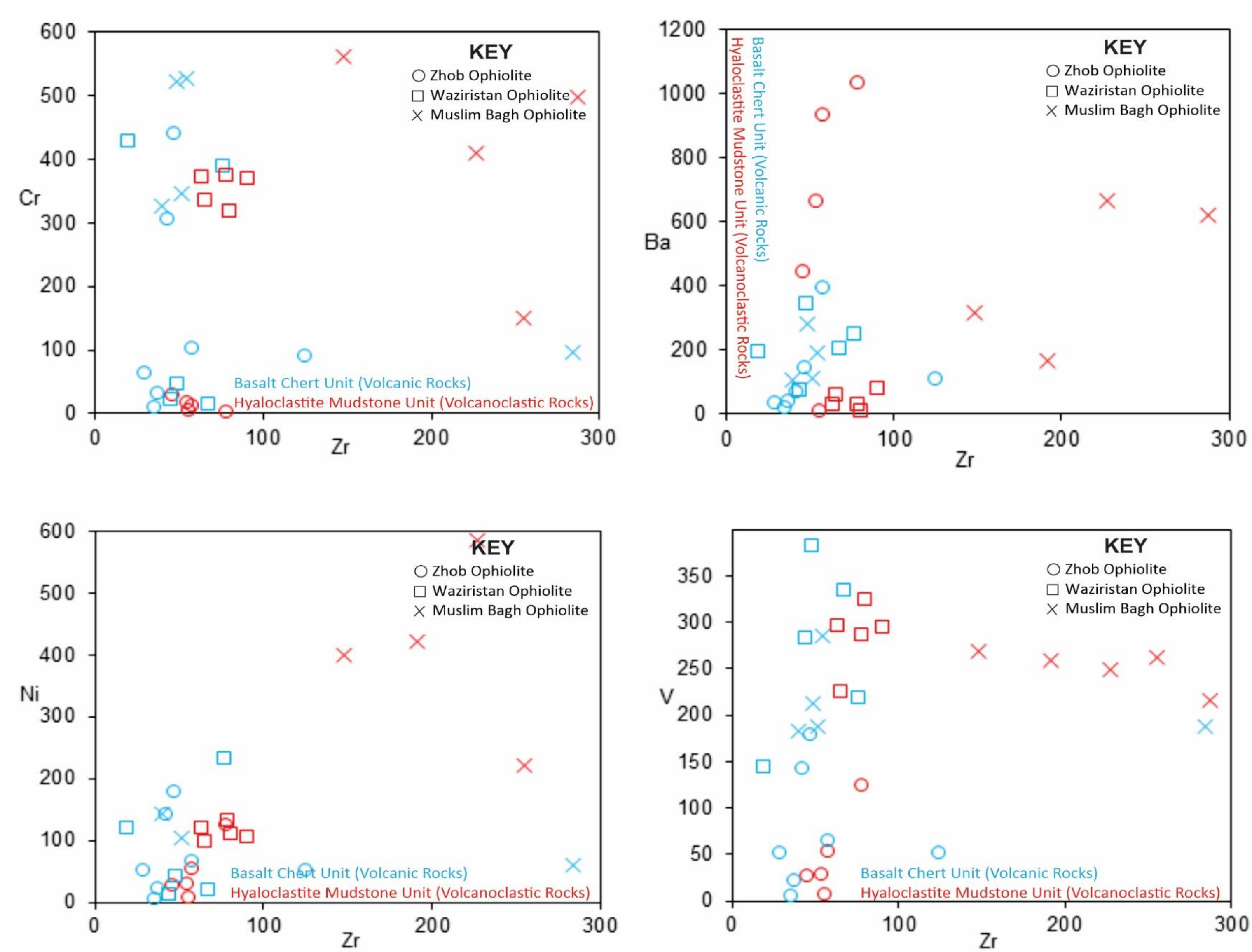
KEY
Zhob Ophiolite
Waziristan Ophiolite
Muslim Bagh Ophiolite
Cr
Zr
Basalt Chert Unit (Volcanic Rocks)
Hyaloclastite Mudstone Unit (Volcanoclastic Rocks)
Ba
Ni
V
0
100
200
300
400
500
600
800
1000
1200
50
150
250
350

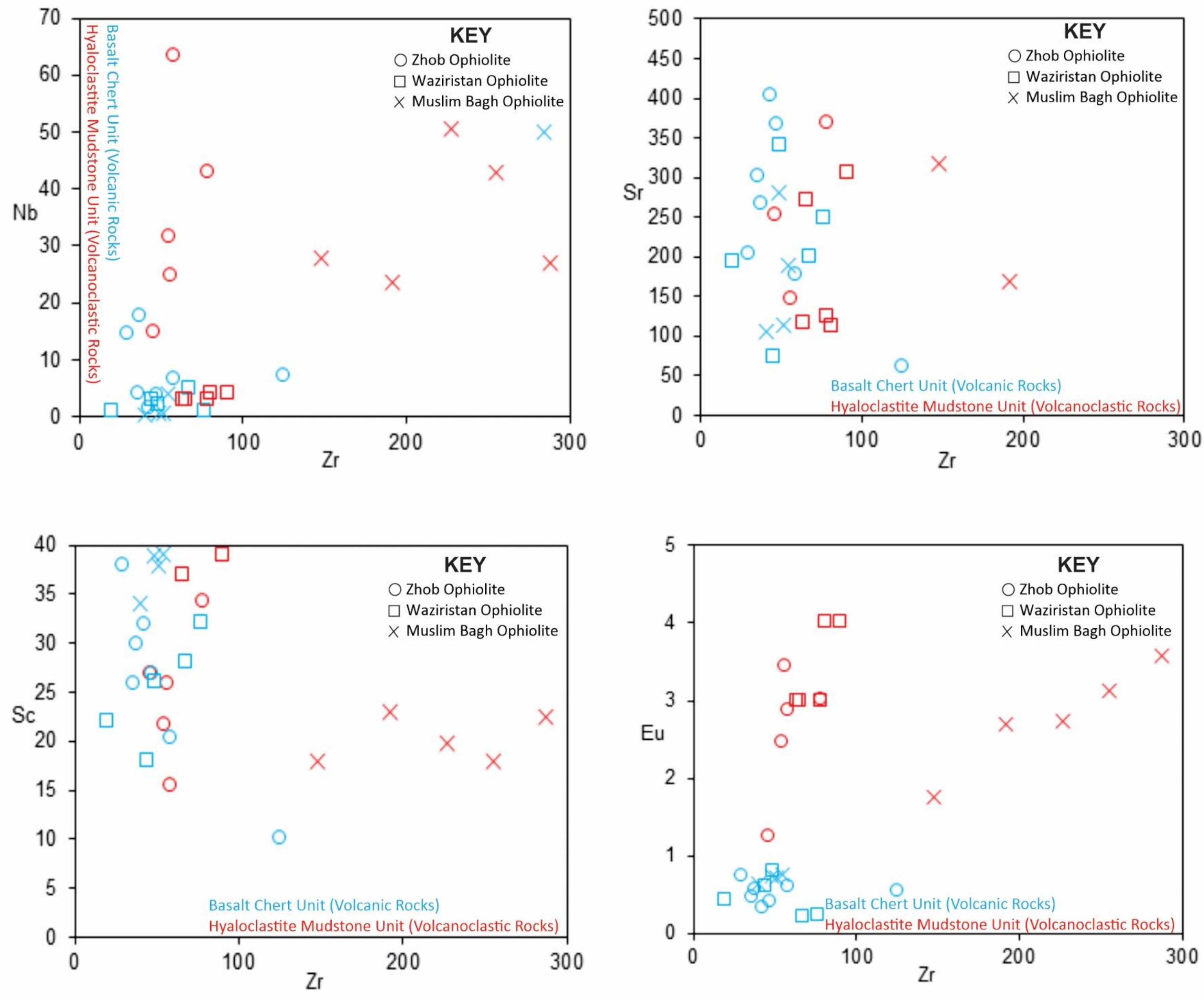
Nb
Zr
Basalt Chert Unit (Volcanic Rocks)
Hyaloclastite Mudstone Unit (Volcanoclastic Rocks)
KEY
Zhob Ophiolite
Waziristan Ophiolite
Muslim Bagh Ophiolite
Sr
Zr
KEY
Zhob Ophiolite
Waziristan Ophiolite
Muslim Bagh Ophiolite
Basalt Chert Unit (Volcanic Rocks)
Hyaloclastite Mudstone Unit (Volcanoclastic Rocks)
Sc
Zr
KEY
Zhob Ophiolite
Waziristan Ophiolite
Muslim Bagh Ophiolite
Basalt Chert Unit (Volcanic Rocks)
Hyaloclastite Mudstone Unit (Volcanoclastic Rocks)
Eu
Zr
KEY
Zhob Ophiolite
Waziristan Ophiolite
Muslim Bagh Ophiolite
Basalt Chert Unit (Volcanic Rocks)
Hyaloclastite Mudstone Unit (Volcanoclastic Rocks)

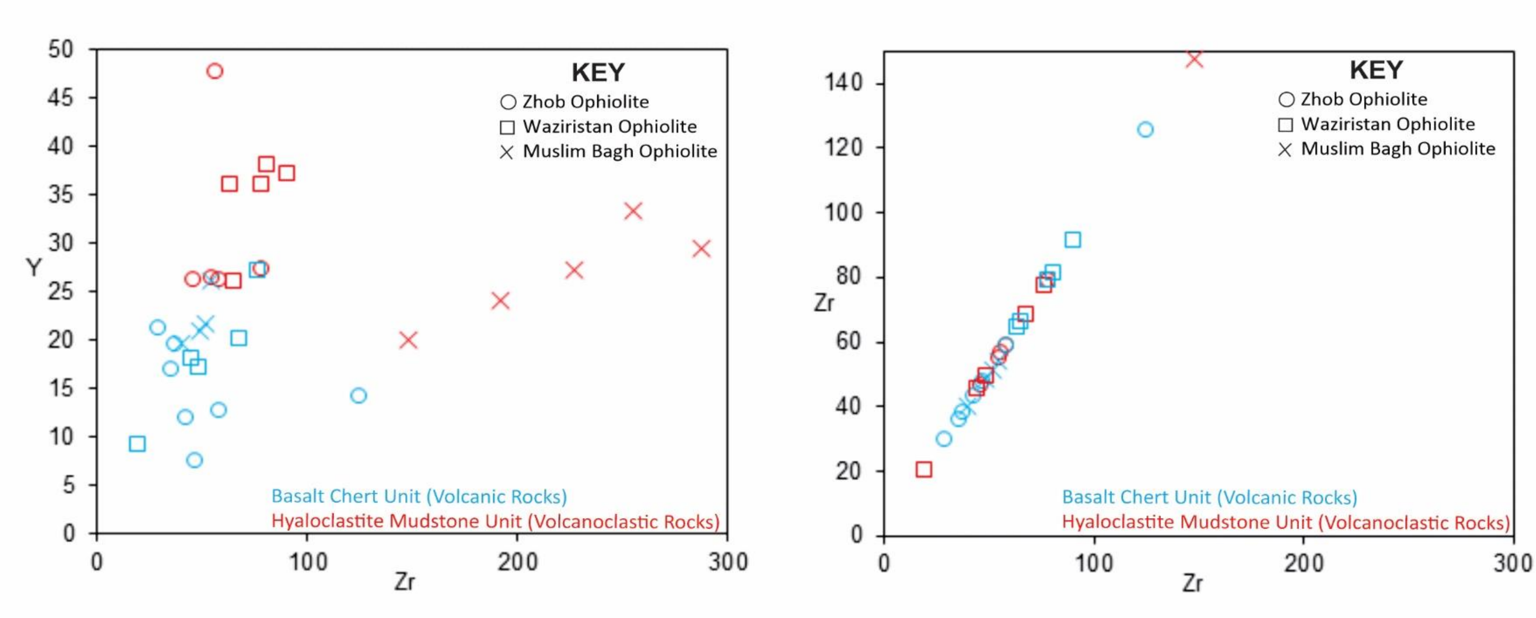

KEY
Zhob Ophiolite
Waziristan Ophiolite
Muslim Bagh Ophiolite
Basalt Chert Unit (Volcanic Rocks)
Hyaloclastite Mudstone Unit (Volcanoclastic Rocks)
Y
Zr
KEY
Zhob Ophiolite
Waziristan Ophiolite
Muslim Bagh Ophiolite
Basalt Chert Unit (Volcanic Rocks)
Hyaloclastite Mudstone Unit (Volcanoclastic Rocks)
Zr
Zr

Figure 7

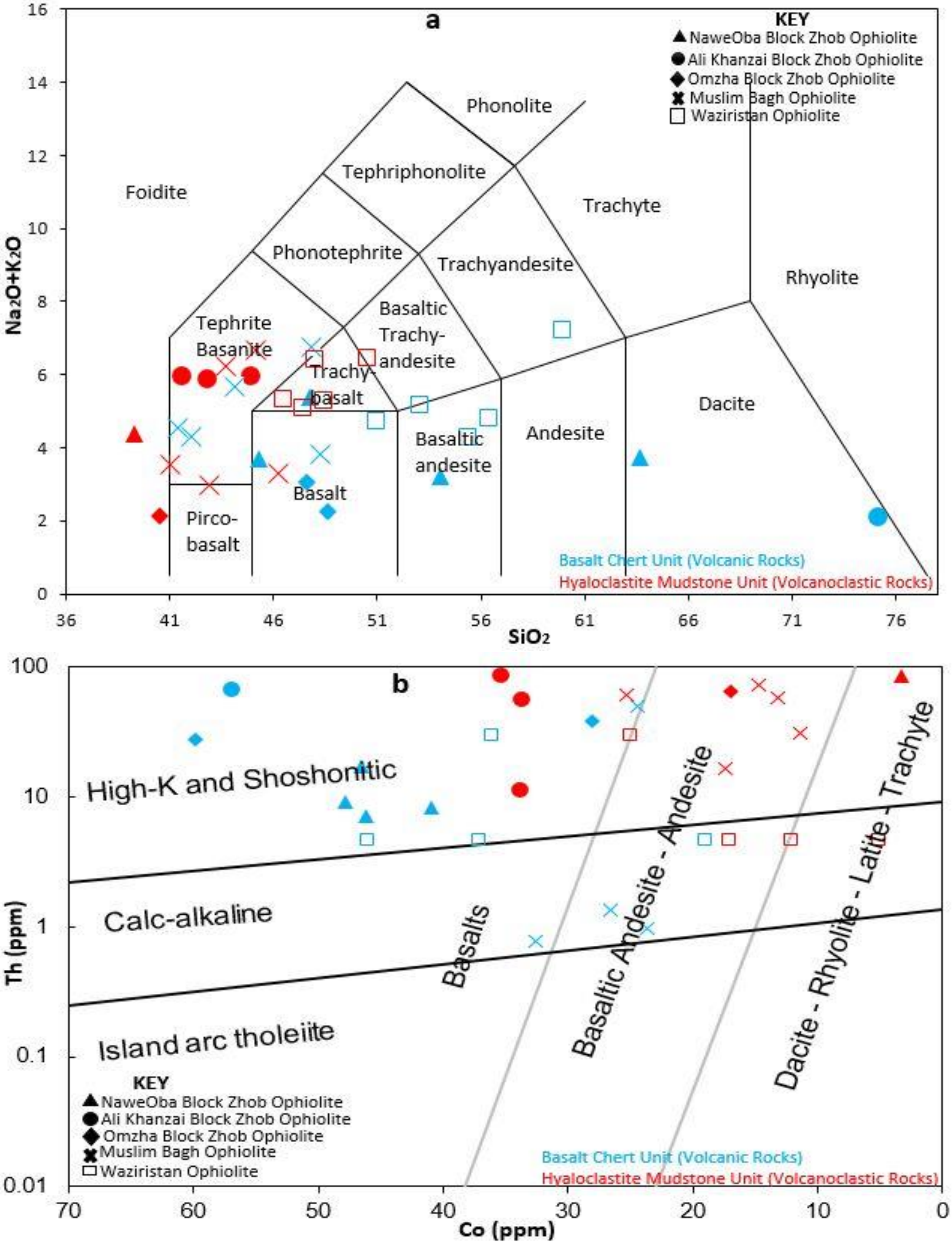
a
KEY
NaweOba Block Zhob Ophiolite
Ali Khanzai Block Zhob Ophiolite
Omzha Block Zhob Ophiolite
Muslim Bagh Ophiolite
Waziristan Ophiolite
Phonolite
Tephriphonolite
Foidite
Trachyte
Phonotephrite
Trachyandesite
Rhyolite
Basaltic Trachy-andesite
Tephrite Basanite
Trachy-basalt
Dacite
Basaltic andesite
Andesite
Basalt
Pirco-basalt
Basalt Chert Unit (Volcanic Rocks)
Hyaloclastite Mudstone Unit (Volcanoclastic Rocks)
Na2O+K2O
SiO2
b
High-K and Shoshonitic
Calc-alkaline
Island arc tholeiite
Basalts
Basaltic Andesite - Andesite
Dacite - Rhyolite - Latite - Trachyte
KEY
NaweOba Block Zhob Ophiolite
Ali Khanzai Block Zhob Ophiolite
Omzha Block Zhob Ophiolite
Muslim Bagh Ophiolite
Waziristan Ophiolite
Basalt Chert Unit (Volcanic Rocks)
Hyaloclastite Mudstone Unit (Volcanoclastic Rocks)
Th (ppm)
Co (ppm)

Figure 8

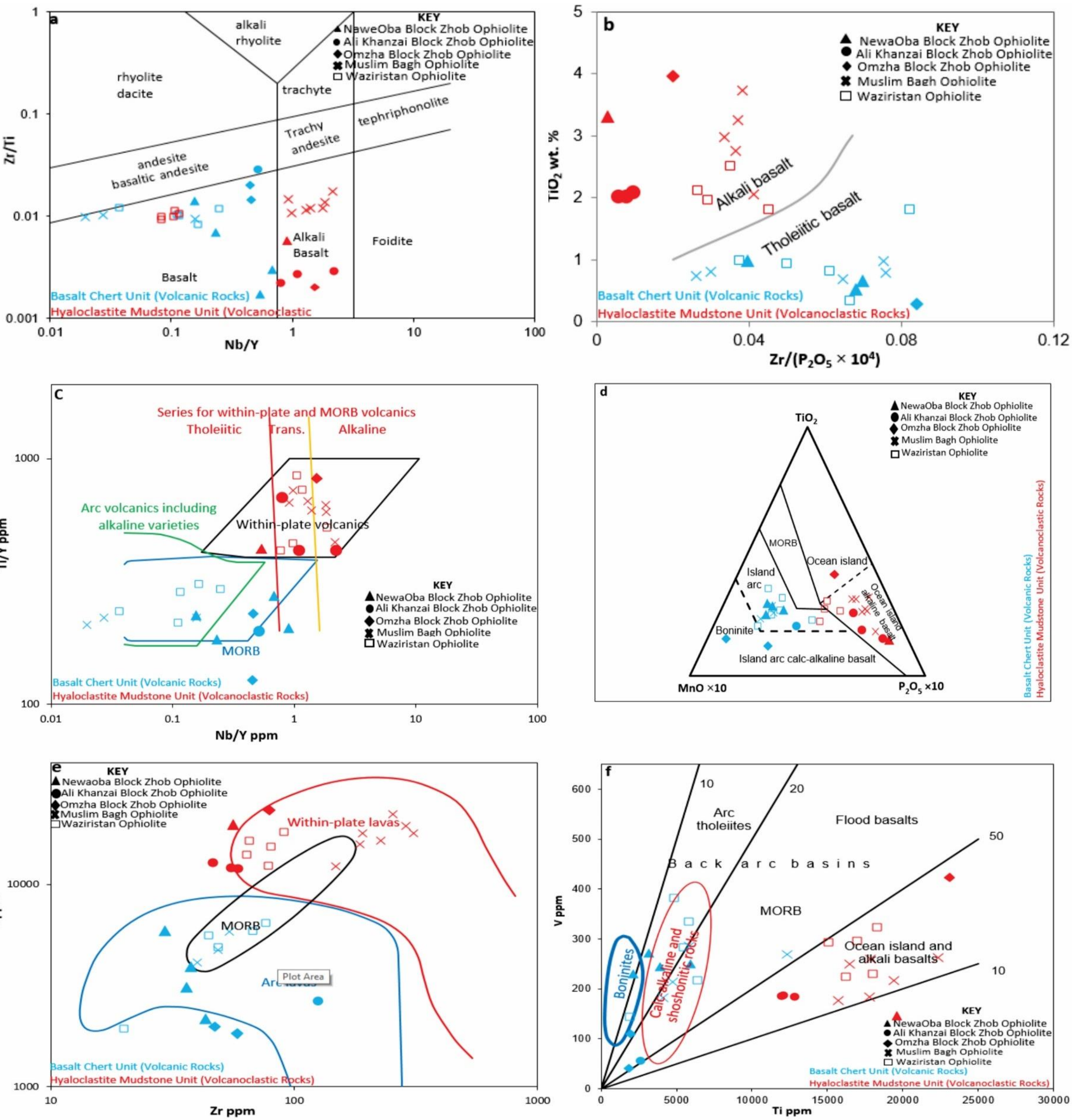
a
KEY
NaweOba Block Zhob Ophiolite
Ali Khanzai Block Zhob Ophiolite
Omzha Block Zhob Ophiolite
Muslim Bagh Ophiolite
Waziristan Ophiolite
alkali rhyolite
rhyolite dacite
trachyte
tephriphonolite
Trachy andesite
andesite basaltic andesite
Alkali Basalt
Foidite
Basalt
Basalt Chert Unit (Volcanic Rocks)
Hyaloclastite Mudstone Unit (Volcanoclastic
Zr/Ti
Nb/Y
b
Alkali basalt
Tholeiitic basalt
TiO2 wt. %
Zr/(P2O5 × 10^4)
Hyaloclastite Mudstone Unit (Volcanoclastic Rocks)
C
Series for within-plate and MORB volcanics
Tholeiitic
Trans.
Alkaline
Arc volcanics including alkaline varieties
Within-plate volcanics
MORB
Ti/Y ppm
Nb/Y ppm
d
TiO2
MORB
Ocean island
Island arc
Ocean island alkaline basalt
Boninite
Island arc calc-alkaline basalt
MnO ×10
P2O5 ×10
e
Newaoba Block Zhob Ophiolite
Within-plate lavas
Arc lavas
Plot Area
Ti ppm
Zr ppm
f
Arc tholeiites
Flood basalts
Back arc basins
Ocean island and alkali basalts
Boninites
Calc-alkaline and shoshonitic rocks
V ppm

Figure 9

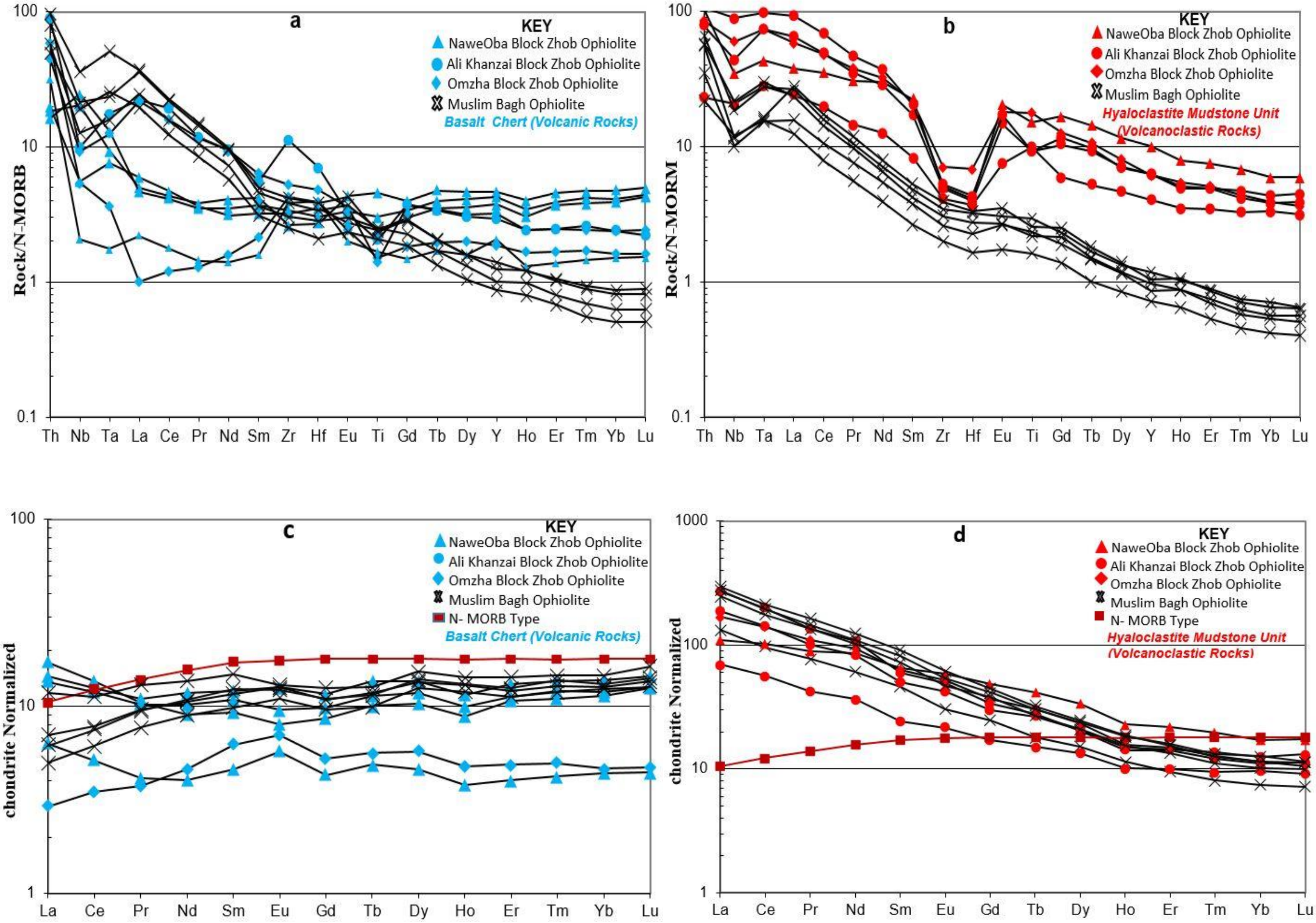
a
KEY
NaweOba Block Zhob Ophiolite
Ali Khanzai Block Zhob Ophiolite
Omzha Block Zhob Ophiolite
Muslim Bagh Ophiolite
Basalt Chert (Volcanic Rocks)
Rock/N-MORB
100
10
1
0.1
Th Nb Ta La Ce Pr Nd Sm Zr Hf Eu Ti Gd Tb Dy Y Ho Er Tm Yb Lu
b
KEY
NaweOba Block Zhob Ophiolite
Ali Khanzai Block Zhob Ophiolite
Omzha Block Zhob Ophiolite
Muslim Bagh Ophiolite
Hyaloclastite Mudstone Unit
(Volcanoclastic Rocks)
Rock/N-MORM
100
10
1
0.1
Th Nb Ta La Ce Pr Nd Sm Zr Hf Eu Ti Gd Tb Dy Y Ho Er Tm Yb Lu
c
KEY
NaweOba Block Zhob Ophiolite
Ali Khanzai Block Zhob Ophiolite
Omzha Block Zhob Ophiolite
Muslim Bagh Ophiolite
N- MORB Type
Basalt Chert (Volcanic Rocks)
chondrite Normalized
100
10
1
La Ce Pr Nd Sm Eu Gd Tb Dy Ho Er Tm Yb Lu
d
KEY
NaweOba Block Zhob Ophiolite
Ali Khanzai Block Zhob Ophiolite
Omzha Block Zhob Ophiolite
Muslim Bagh Ophiolite
N- MORB Type
Hyaloclastite Mudstone Unit
(Volcanoclastic Rocks)
chondrite Normalized
1000
100
10
1
La Ce Pr Nd Sm Eu Gd Tb Dy Ho Er Tm Yb Lu

Figure 10

Table

Table 1

Sample No	NB02	NB42	NB44	NB28	NB39	AK08	AK10	AK29	AK44	OMZ10	OMZ11	OMZ39
Rock Type	Basalt	Basalt	Basalt	Hyalocla	Basalt	Hyalocla	Basalt	Hyalocla	Hyalocla	Basalt	Basalt	Hyalocla
SiO_2	63.71	45.34	54.09	39.35	47.80	41.63	75.22	42.85	44.99	47.63	48.64	40.55
TiO_2	0.52	0.98	0.66	3.31	0.37	2.09	0.45	2.02	2.02	0.33	0.29	3.95
Al_2O_3	13.23	10.67	11.03	14.83	12.42	12.48	6.66	13.34	14.80	15.45	5.98	11.80
Fe_2O_3	8.87	7.16	7.90	11.69	7.23	6.21	3.75	7.63	9.57	9.61	2.51	14.22
MnO	0.09	0.18	0.15	0.21	0.11	0.23	0.11	0.19	0.15	0.17	0.16	0.18
MgO	2.80	3.43	3.07	4.57	2.30	2.36	1.74	2.81	3.43	12.14	1.88	9.44
CaO	4.34	14.01	9.96	9.65	11.82	15.78	3.76	14.16	12.39	7.49	19.57	11.79
Na_2O	3.67	3.25	3.08	4.34	5.36	3.75	0.30	3.19	2.61	2.38	0.97	2.00
K_2O	0.04	0.42	0.13	0.03	0.01	2.20	1.77	2.66	3.32	0.67	1.26	0.10
P_2O_5	0.05	0.07	0.05	1.79	0.02	0.48	0.08	0.69	0.99	0.02	0.07	0.39
CR_2O_3	0.00	0.01	0.00	0.00	0.04	0.00	0.01	0.00	0.00	0.06	0.01	0.00
LOI	2.01	14.03	8.77	9.19	11.00	12.52	4.93	9.21	5.17	3.58	17.50	5.12
Total	99.34	99.55	98.90	98.95	98.50	99.72	98.78	98.76	99.43	99.54	98.85	99.54
Sc	25.8	38.0	29.9	25.9	31.9	26.9	10.0	21.6	15.4	26.9	20.2	34.2
V	272.4	246.2	241.5	153.3	226.2	178.7	56.3	173.4	180.7	108.7	39.9	420.9
Cr	7.8	62.4	29.3	2.6	304.1	28.6	89.7	15.7	11.4	439.6	100.6	1.4
Co	19.1	28.7	21.4	66.1	22.2	35.4	11.2	34.6	37.4	40.8	7.1	48.9
Ni	4.7	51.0	21.3	6.6	141.3	25.3	51.1	28.4	53.1	177.6	63.8	123.3
Cu	56.1	12.1	30.7	33.9	58.0	34.2	49.3	37.2	49.4	100.9	9.8	299.6
Zn	87.8	32.4	47.0	106.4	43.3	61.8	47.2	79.0	97.6	112.1	33.5	71.8
Sr	300.9	202.9	267.4	146.5	402.1	252.7	60.9	787.0	1464.3	366.4	176.0	368.9
Y	16.8	21.1	19.4	47.5	11.8	26.0	14.1	26.3	26.1	7.4	12.6	27.1
Zr	36.7	30.7	39.8	53.0	44.7	41.7	122.8	51.7	59.7	48.9	57.3	77.9
Ba	16.9	35.2	41.0	8.0	62.7	434.7	119.7	675.4	993.0	147.3	412.5	1064.6
V	271.4	250.8	243.8	146.3	229.2	183.8	54.9	187.1	185.1	110.3	41.3	423.0
Cr	10.1	64.9	30.1	2.6	178.8	18.8	84.0	16.0	12.7	439.4	97.2	1.7
Co	22.1	29.0	23.8	66.7	23.4	36.1	13.0	36.2	34.5	41.9	10.2	53.1

Ni	5.1	58.6	23.4	10.8	90.5	16.8	51.2	33.3	53.4	176.1	62.8	120.1
Cu	51.1	10.4	31.0	35.2	60.8	32.3	48.3	40.7	51.1	104.1	9.0	304.8
Zn	83.2	35.6	46.2	108.2	46.8	72.6	46.6	79.3	95.9	109.6	33.3	69.9
Ga	10.6	5.7	7.4	17.7	4.1	7.8	9.2	17.0	20.9	9.3	6.9	23.6
Rb	1.1	6.4	2.0	1.1	0.6	11.7	49.0	28.4	38.0	10.7	41.6	2.2
Sr	312.1	217.4	268.7	137.0	260.5	178.8	59.9	825.7	1461.6	371.5	189.1	374.4
Y	17.0	21.2	19.2	45.7	9.4	18.5	13.5	28.7	28.4	8.5	14.6	27.8
Zr	35.9	29.4	37.7	56.5	43.1	46.2	125.2	54.9	58.6	47.5	58.6	78.8
Nb	3.95	14.47	17.52	24.81	1.47	14.81	7.07	31.56	63.25	3.85	6.57	42.77
Cs	0.02	0.13	0.03	0.01	0.00	0.07	1.64	0.16	0.17	0.44	1.48	0.16
Ba	15.6	33.4	37.3	6.5	64.7	440.8	106.7	658.5	927.7	141.6	393.0	1027.8
La	4.08	3.44	3.21	26.01	1.50	16.54	15.22	44.43	63.98	0.69	14.97	39.98
Ce	8.32	7.69	7.33	62.81	3.15	34.74	34.17	87.70	122.06	2.14	28.29	86.03
Pr	1.00	1.05	0.98	8.47	0.40	4.02	3.25	9.63	12.88	0.36	3.18	10.38
Nd	4.23	5.52	4.76	40.47	1.89	17.05	12.70	38.65	50.42	2.15	12.61	43.82
Sm	1.42	1.86	1.65	9.94	0.71	3.69	2.47	7.63	9.11	0.96	2.80	9.61
Eu	0.46	0.73	0.56	3.44	0.33	1.25	0.54	2.47	2.88	0.41	0.60	3.01
Gd	1.77	2.38	2.03	9.93	0.88	3.53	2.23	6.16	6.97	1.09	2.19	7.51
Tb	0.38	0.51	0.43	1.55	0.18	0.56	0.37	1.00	1.05	0.21	0.37	1.14
Dy	2.62	3.45	3.01	8.49	1.17	3.41	2.25	5.22	5.15	1.46	2.31	5.91
Ho	0.50	0.66	0.57	1.30	0.21	0.57	0.40	0.84	0.80	0.27	0.40	0.89
Er	1.77	2.17	1.86	3.62	0.67	1.66	1.18	2.37	2.35	0.81	1.18	2.45
Tm	0.28	0.35	0.31	0.51	0.11	0.24	0.19	0.35	0.31	0.13	0.18	0.33
Yb	1.93	2.35	2.03	2.92	0.75	1.63	1.18	2.13	1.88	0.79	1.17	1.94
Lu	0.32	0.37	0.32	0.44	0.11	0.23	0.17	0.33	0.29	0.12	0.18	0.27
Hf	1.08	0.84	0.95	1.27	1.22	1.15	2.18	1.22	1.33	1.21	1.48	2.12
Ta	0.31	0.38	0.53	1.77	0.07	1.14	0.72	3.02	3.99	0.15	0.51	3.03
Pb	1.76	1.63	3.54	6.64	1.28	1.31	6.13	3.44	4.96	1.21	8.58	8.88
Th	1.69	1.56	1.39	8.80	2.69	1.97	7.53	6.64	9.08	4.90	3.82	7.18
U	0.43	0.19	0.30	0.72	0.12	2.10	0.77	2.58	2.00	0.05	1.17	1.33

Note: LOI = Loss on ignition at 1000C, Fe_2O_3 = Total Iron, Hyalocla = Hyaloclastite

Table 1 ***continue***

Rock Type	***Bbc**	***Bbc**	***Bbc**	***Bbc**	***Bbc**	***Bbc**	***Bbc**	***Bbc**	***Bhm**	***Bhm**	***Bhm**	***Bhm**	***Bhm**	***Bhm**
Sample No	**C65**	**C63**	**C123**	**C19**	**C18**	**C85**	**C62**	**C13C**	**C15**	**C64**	**C126**	**C58**	**C61**	**C59**
SiO_2	44.09	48.24	47.79	41.37	47.09	43.78	60.03	39.25	46.19	41.00	43.65	45.13	42.88	34.12
TiO_2	2.97	0.98	0.79	0.69	0.79	3.13	1.11	3.17	2.06	2.75	3.72	2.98	3.24	2.71
Al_2O_3	13.36	15.05	13.47	12.07	12.88	14.52	14.09	12.05	8.72	10.86	13.04	9.64	11.03	9.01
Fe_2O_3	13.03	9.28	9.42	8.57	8.97	11.73	9.99	11.52	10.67	11.39	12.08	12.42	12.08	11.08
MnO	0.20	0.17	0.20	0.14	0.16	0.17	0.13	0.18	0.10	0.12	0.17	0.07	0.15	0.15
MgO	8.05	8.18	7.75	6.87	7.27	5.87	2.30	8.39	7.85	7.79	7.23	7.94	10.61	11.55
CaO	7.93	10.28	10.29	17.13	11.85	10.77	6.63	15.21	13.72	16.42	10.12	11.20	12.90	15.27
Na_2O	2.01	3.25	6.49	4.49	5.92	2.15	5.93	2.35	2.87	2.29	1.06	6.40	1.24	1.71
K_2O	3.67	0.60	0.30	0.07	0.04	2.73	0.09	0.99	0.44	1.26	5.21	0.31	1.75	1.33
P_2O_5	1.18	0.07	0.06	0.06	0.07	0.82	0.22	0.80	0.36	0.62	0.67	0.57	0.78	0.51
LOI	3.56	3.71	2.63	7.85	5.29	3.05	0.56	6.57	6.40	5.32	3.56	3.70	3.55	11.95
Total	100.38	99.92	99.27	99.38	100.40	99.07	101.22	100.83	99.60	100.12	100.92	100.68	100.57	99.70
Sc	12.6	39.2	38.9	34.1	37.9	15.2	25.9	19.9	17.9	19.8	17.9	23.0	22.5	23.1
V	183.3	285.2	213.4	182.5	187.1	187.5	290.8	184.9	269.6	249.9	262.6	259.7	216.0	111.7
Cr	38.2	526.9	523.0	326.2	346.2	96.0	1.7	371.9	562.4	409.1	149.7	796.9	497.2	740.0
Co	55.9	43.3	46.3	37.4	39.2	55.4	18.6	53.8	52.6	44.6	55.3	58.5	56.7	54.0
Ni	193.7	1516.2	1089.8	142.3	103.8	59.1	84.8	1775.2	400.9	584.3	221.0	422.6	724.5	968.2
Cu	34.9	35.0	30.5	56.6	48.9	33.6	54.2	58.3	36.4	31.7	76.5	52.9	79.9	47.6
Zn	180.4	106.7	143.0	75.5	81.6	127.4	92.0	166.4	124.6	94.1	213.7	117.2	113.3	118.2

Ga	24.2	16.6	13.5	16.8	14.7	24.8	17.7	20.8	16.5	21.5	26.9	14.4	20.2	18.1
Sr	886.0	189.6	281.8	105.0	112.9	2390.3	107.6	562.2	317.4	662.9	1284.9	168.1	618.8	195.9
Y	39.0	26.0	20.9	19.5	21.6	35.0	28.2	27.9	20.0	27.1	33.3	24.0	29.4	23.0
Zr	310.0	54.3	48.7	40.1	51.4	283.9	83.1	225.1	147.8	227.1	255.0	191.6	287.4	196.9
Nb	84.05	4.09	0.57	0.39	0.47	49.99	2.37	29.54	27.82	50.46	42.94	23.65	26.97	23.34
Ba	3737.0	123.1	124.9	20.7	49.8	727.1	48.9	415.3	277.6	381.6	1521.3	775.1	1569.5	176.5
La	92.96	2.81	1.67	1.18	1.47	88.70	11.21	61.79	31.37	58.85	65.76	39.38	69.72	45.60
Ce	169.24	6.92	4.78	3.77	4.59	164.30	21.98	117.28	58.92	107.51	118.96	79.10	131.07	92.10
Pr	19.77	1.24	0.91	0.73	0.90	19.08	3.04	13.99	7.33	12.80	13.89	9.96	15.57	10.87
Nd	70.56	6.36	4.97	4.20	5.05	68.79	13.37	52.27	28.62	47.73	51.51	39.67	57.82	42.18
Sm	13.16	2.27	1.77	1.51	1.90	12.05	3.36	9.62	6.99	11.08	12.58	9.89	13.92	9.90
Eu	4.37	0.76	0.74	0.64	0.71	3.78	1.13	3.04	1.76	2.74	3.13	2.70	3.57	2.46
Gd	10.67	2.59	2.23	1.97	2.26	10.46	3.60	8.37	5.06	7.85	8.49	7.01	9.22	6.93
Tb	1.38	0.47	0.44	0.37	0.43	1.38	0.63	1.13	0.67	1.00	1.13	0.98	1.20	0.94
Dy	7.18	3.92	3.44	3.18	3.54	7.21	4.74	6.00	3.83	5.32	6.05	5.29	6.31	5.05
Ho	1.22	0.81	0.74	0.68	0.74	1.23	0.98	1.00	0.65	0.88	1.04	0.88	1.06	0.83
Er	3.13	2.38	2.01	1.86	2.06	3.02	2.65	2.38	1.57	2.22	2.62	2.06	2.55	2.00
Tm	0.43	0.37	0.33	0.30	0.35	0.41	0.45	0.31	0.21	0.28	0.34	0.26	0.32	0.26
Yb	2.65	2.49	2.15	2.10	2.23	2.49	2.98	1.91	1.27	1.72	2.15	1.62	1.96	1.54
Lu	0.41	0.41	0.35	0.32	0.36	0.37	0.48	0.29	0.18	0.25	0.29	0.23	0.29	0.23
Hf	7.79	1.46	1.31	1.15	1.32	6.95	2.23	5.85	3.38	5.66	6.53	4.66	6.82	4.70
Ta	6.76	0.24	0.03	0.03	0.03	3.08	0.12	2.09	2.05	3.96	3.64	2.05	2.18	2.25
Pb	9.04	7.37	4.32	3.48	5.15	11.07	5.03	6.29	5.15	12.37	12.39	5.74	8.97	5.32
Th	11.60	0.39	0.31	0.26	0.32	9.57	1.66	6.86	2.60	6.95	7.94	4.17	6.67	4.91

U	3.07	0.08	0.05	0.07	0.10	3.87	0.40	1.62	0.71	1.28	2.27	1.07	1.98	1.73

Note: LOI = Loss on ignition at 1000C, Fe_2O_3 = Total Iron, Bbc=Basalt Chert, Bhm= Hyaloclastite Mudstone

Table 1 *continue*

Rock Type	**Basalt	**Basalt	**Basalt	**Basalt	**Basalt	**Hyalocla	**Hyalocla	**Hyalocla	**Hyalocla	**Hyalocla
Samples Name	**WV 1**	**WV 2**	**WV 3**	**WV 4**	**WV 5**	**WVV2**	**WVV11**	**WVV12**	**WVV55**	**WVV125**
SiO_2	55.39	56.4	59.97	50.99	53.08	48.02	46.5	48.45	47.44	50.56
TiO_2	0.81	0.92	0.32	1.07	0.97	1.34	1.16	1.39	1.04	1.35
Al_2O_3	15.6	15.77	17.17	16.61	15.84	16.33	17.39	15.26	18.56	15.69
Fe_2O_3	11.08	9.92	8.73	9.08	11.27	11.68	10.54	12.14	8.46	10.88
MnO	0.25	0.17	0.07	0.15	0.16	0.12	0.18	0.15	0.15	0.12
MgO	5.05	3.32	1.58	7.12	4.43	2.74	2.56	3.18	6.14	4.13
CaO	2.85	5.37	3.66	8	6.54	9.85	11.03	9.66	10.76	6.95
Na_2O	4.25	4.4	7.15	2.81	3.91	5.37	5.28	5.25	3.2	5.94
K_2O	0.04	0.4	0.06	1.91	1.26	1.06	0.03	0.04	1.4	0.5
P_2O_5	0.08	0.09	0.03	0.05	0.18	0.27	0.24	0.23	0.08	0.2
LOI	4.6	3.35	1.26	2.21	2.36	4.26	5.11	4.25	3.65	3.69
Sum	100	100	100	100	100	100	100	100	100	100
Nb	2	3	1	1	5	3	3	4	3	4
Zr	49	45	20	77	68	79	64	81	66	91
Y	17	18	9	27	20	36	36	38	26	37
Sr	340	73	193	248	199	124	115	112	271	306

Rb	3	7	4	60	20	4	4	3	8	10
Zn	663	95	56	59	85	124	114	133	62	124
Ni	40	10	119	232	18	132	118	110	97	103
Cr	45	20	426	388	13	373	371	317	334	368
V	382	282	143	217	334	285	296	323	224	293
Ba	26	41	55	212	153	28	27	8	54	74
Cu	174	100	14	11	145	40	22	59	69	46
Co	24	33	53	51	34	58	65	51	53	45
Ce	18	4	11	27	30	bdl	5	10	28	30
Sc	26	18	22	32	28	46	54	46	37	39
Ga	15	16	8	11	16	17	25	17	17	16
Th	0.8	0.6	0.43	0.23	0.2	0.2	0.3	0.6	1.9	0.86
Nd	6	8	8	10	12	bdl	6	9	12	13
Zr/Y	13	3.6	3.2	2.8	3	13	3.6	3.2	2.8	3

Note: LOI = Loss on ignition at 1000C, Fe_2O_3 = Total Iron, Hyalocla = Hyaloclastite